USGS
science for a changing world

RESULTS FROM AIR-INJECTION AND TRACER TESTING IN THE UPPER TIVA CANYON, BOW RIDGE FAULT, AND UPPER PAINTBRUSH CONTACT ALCOVES OF THE EXPLORATORY STUDIES FACILITY, AUGUST 1994 THROUGH JULY 1996, YUCCA MOUNTAIN, NEVADA

U.S. GEOLOGICAL SURVEY

Water-Resources Investigations Report 98–4058

Prepared in cooperation with the
NEVADA OPERATIONS OFFICE,
U.S. DEPARTMENT OF ENERGY, under
Interagency Agreement DE–AI08–97NV12033

DISCLAIMER

Results from Air-Injection and Tracer Testing in the Upper Tiva Canyon, Bow Ridge Fault, and Upper Paintbrush Contact Alcoves of the Exploratory Studies Facility, August 1994 through July 1996, Yucca Mountain, Nevada

by **Gary D. LeCain**

U.S. GEOLOGICAL SURVEY

Water-Resources Investigations Report 98–4058

Prepared in cooperation with the
NEVADA OPERATIONS OFFICE,
U.S. DEPARTMENT OF ENERGY, under
Interagency Agreement DE–AI08–97NV12033

Denver, Colorado
1998

U.S. DEPARTMENT OF THE INTERIOR
BRUCE BABBITT, Secretary

U.S. GEOLOGICAL SURVEY
Thomas J. Casadevall, Acting Director

For additional information write to:

Chief, Earth Science Investigations Program
Yucca Mountain Project Branch
U.S. Geological Survey
Box 25046, Mail Stop 421
Denver Federal Center
Denver, CO 80225-0046

Copies of this report can be purchased from:

U.S. Geological Survey
Information Services
Box 25286
Federal Center
Denver, CO 80225

CONTENTS

Abstract 1
Introduction 2
Test and Analysis Methods 5
Methods and Analysis for Single-Hole Air-Injection Testing 5
Methods and Analysis for Cross-Hole Air-Injection Testing 8
Methods and Analysis for Cross-Hole Tracer Testing 10
Upper Tiva Canyon Alcove 12
Alcove and Borehole Construction 12
Geology 13
Results from Single-Hole Air-Injection Tests 13
Results from Cross-Hole Air-Injection Tests 16
Bow Ridge Fault Alcove 17
Alcove and Borehole Construction 17
Geology 17
Results from Single-Hole Air-Injection Tests 19
Results from Cross-Hole Air-Injection Tests 21
Results from Cross-Hole Tracer Tests 22
Upper Paintbrush Contact Alcove 22
Alcove and Borehole Construction 22
Geology 23
Results from Single-Hole Air-Injection Tests 24
Summary 26
References Cited 28

FIGURES

1. Map showing location of Nevada Test Site and the potential repository at Yucca Mountain 3
2. Diagramatic map showing the Exploratory Studies Facility, upper Tiva Canyon, Bow Ridge Fault, and upper Paintbrush contact alcoves 4
3. Schematic diagram showing single-hole air-injection testing 5
4. Graph showing absolute pressure and times of test 181, upper Paintbrush contact alcove, indicating water redistribution 6
5. Graph showing pressure squared differences and flow rates of tests 182 through 188, upper Paintbrush contact alcove 8
6. Graph showing log-log plot of pressure squared differences and flow rates of tests 182 through 188, upper Paintbrush contact alcove 9
7. Graph showing pressure squared differences divided by the flow rate and flow rates of tests 182 through 188, upper Paintbrush contact alcove, and the y intercept 10
8. Schematic diagram showing cross-hole air-injection testing 11
9. Schematic diagram showing the upper Tiva Canyon alcove and boreholes RBT#1, RBT#2, and RBT#3 12
10. Histograms showing *(A)*, air-injection permeability values and *(B)*, natural logarithm of air-injection permeability values for boreholes RBT#1, RBT#2, and RBT#3 in the upper Tiva Canyon alcove 15
11. Schematic diagram showing the Bow Ridge Fault alcove and boreholes HPF#1 and HPF#2 18
12. Schematic diagram showing Bow Ridge Fault, Bow Ridge Fault alcove, and borehole HPF#1 19
13. Schematic diagram showing upper Paintbrush contact alcove and boreholes RBT#1 and RBT#4 23

TABLES

1. Permeability values and water-redistribution pressures from air-injection testing in borehole RBT#1 located in the crystal-poor upper lithophysal zone of the Tiva Canyon Tuff in the upper Tiva Canyon alcove 13

2. Permeability values and water-redistribution pressures from air-injection testing in borehole RBT#2 located in the crystal-poor upper lithophysal zone of the Tiva Canyon Tuff in the upper Tiva Canyon alcove 14
3. Permeability values and water-redistribution pressures from air-injection testing in borehole RBT#3 located in the crystal-poor upper lithophysal zone of the Tiva Canyon Tuff in the upper Tiva Canyon alcove 14
4. Statistical summary of the permeability values from air-injection testing in boreholes RBT#1, RBT#2, and RBT#3 located in the crystal-poor upper lithophysal zone of the Tiva Canyon Tuff in the upper Tiva Canyon alcove 16
5. Permeability values, water-redistribution pressures, and geologic zones from air-injection testing in borehole HPF#1 located in the Bow Ridge Fault alcove 20
6. Statistical summary of the permeability values from air-injection testing in borehole HPF#1 located in the Bow Ridge Fault alcove, by geologic zone 20
7. Permeability and porosity values from cross-hole air-injection testing in boreholes HPF#1 and HPF#2 located in the Bow Ridge Fault alcove 21
8. Test results from cross-hole tracer testing in boreholes HPF#1 and HPF#2 located in the Bow Ridge Fault alcove 22
9. Permeability values, water-redistribution pressures, and geologic zones from air-injection testing in borehole RBT#1 located in the upper Paintbrush contact alcove 25
10. Permeability values, water-redistribution pressures, and geologic zones from air-injection testing in borehole RBT#4 located in the upper Paintbrush contact alcove 25
11. Statistical summary of the permeability values for the upper Paintbrush contact alcove and for the surface-based testing program, by geologic zone 26

CONVERSION FACTORS AND VERTICAL DATUM

Multiply	By	To Obtain
atmosphere (atm)	14.696	pound-force per square inch
centimeter (cm	0.3937	inch
cubic meter (m^3)	35.314	cubic foot
cubic meter per second (m^3/s)	15,852.0	gallon per minute
kilogram per cubic meter (kg/m^3)	0.062	pound per cubic foot
kilometer (km)	0.6214	mile
kilopascals (kPa)	0.145	pound per square inch
liter (L)	0.264	gallon
meter (m)	3.281	foot
meter per second (m/s)	196.850	foot per minute
meter per second squared (m/s^2)	1.18×10^{-4}	foot per minute squared
meter squared (m^2)	10.76	square foot
second per meter squared (s/m^2)	---	
part per million (ppm)	---	
pascal (Pa)	1.45×10^{-4}	pound per square inch
pascal squared (Pa^2)	2.1×10^{-8}	pound per square inch squared
pascal second (Pa*s)	10.0	poise
standard liter per minute (sLpm)*	0.2642	gallons per minute

* In this report, the term "standard" means a measurement taken at a temperature of 0 degrees Celsius and atmospheric pressure of 101.3 kilopascals.

Temperature in degrees Celsius (°C) may be converted to degrees Fahrenheit (°F) as follows:
$°F = (1.8 \times °C) + 32$

The permeability equations use degrees Kelvin. To convert degrees Kelvin (K) to degrees Fahrenheit (°F) use the following formula:
$°F = 9/5(K) - 459.67$

Sea level: In this report "sea level" refers to the National Geodetic Vertical Datum of 1929 (NGVD of 1929)—a geodetic datum derived from a general adjustment of the first-order level nets of both the United States and Canada, formerly called Sea Level Datum of 1929.

Results from Air-Injection and Tracer Testing in the Upper Tiva Canyon, Bow Ridge Fault, and Upper Paintbrush Contact Alcoves of the Exploratory Studies Facility, August 1994 through July 1996, Yucca Mountain, Nevada

By Gary D. LeCain

Abstract

Air-injection and tracer testing were conducted in the upper Tiva Canyon, Bow Ridge Fault, and upper Paintbrush contact alcoves in the Exploratory Studies Facility at Yucca Mountain, Nevada, from August 1994 to July 1996. The study was conducted by the U.S. Geological Survey, in cooperation with the U.S. Department of Energy.

The upper Tiva Canyon alcove is located in the crystal-poor upper lithophysal zone of the Tiva Canyon Tuff. Permeability values from single-hole testing ranged from 0.2×10^{-12} to 85.0×10^{-12} meter squared (m^2). The arithmetic mean was 28.6×10^{-12} m^2 and the geometric mean was 16.0×10^{-12} m^2. Water-redistribution pressures of the crystal-poor upper lithophysal zone of the Tiva Canyon Tuff were as low as less than 4.5 kilopascals. Comparison of the upper Tiva Canyon alcove permeability values of the upper lithophysal zone to the surface-based permeability values of the lower lithophysal and lower nonlithophysal zones indicated that, at shallow depths and at the scale of testing, the Tiva Canyon Tuff is nearly isotropic. Cross-hole pneumatic testing was not successful due to the caving and high rugosity of the boreholes.

The Bow Ridge Fault alcove is located in the crystal-poor middle nonlithophysal zone of the Tiva Canyon Tuff on the east side (footwall) of the Bow Ridge Fault. Boreholes penetrated the crystal-poor middle nonlithophysal zone and the crystal-poor lower lithophysal zone of the Tiva Canyon Tuff, the Bow Ridge Fault zone, and the pre-Rainier Mesa tuff. Permeability values from single-hole testing of the crystal-poor middle nonlithophysal zone of the Tiva Canyon Tuff ranged from 6.0×10^{-12} to 26.4×10^{-12} m^2. The arithmetic mean was 13.9×10^{-12} m^2 and the geometric mean was 12.2×10^{-12} m^2. Permeability values from single-hole testing of the crystal-poor lower lithophysal zone of the Tiva Canyon Tuff ranged from 0.6×10^{-12} to 2.0×10^{-12} m^2. The arithmetic mean was 1.3×10^{-12} m^2 and the geometric mean was 1.2×10^{-12} m^2. The three permeability values of the Bow Ridge Fault zone ranged from 8.0×10^{-12} to 15.8×10^{-12} m^2. The two permeability values from the pre-Rainier Mesa tuff were 41.3×10^{-12} m^2 and 22.0×10^{-12} m^2. Water-redistribution pressures of the middle nonlithophysal and lower lithophysal zones were as low as less than 5.6 kilopascals. Cross-hole permeability values were within 2 to 3 times the single-hole results. The porosity estimates of the Bow Ridge fault zone were 0.13 and 0.20, and for the pre-Rainier Mesa tuff, 0.27. Comparison of the Bow Ridge Fault alcove permeability values of the middle nonlithophysal zone with the surface-based

permeability values of the lower lithophysal and lower nonlithophysal zones indicated that the Tiva Canyon Tuff is isotropic. Comparison of the Bow Ridge Fault alcove permeability values of the lower lithophysal zone with the surface-based permeability values of the lower lithophysal zone indicated that the lower lithophysal zone is anisotropic with a horizontal to vertical ratio of as much as 29:1. An alternate interpretation is that the indicated anisotropy may be due to the small surface-based data base. Cross-hole tracer tests indicated tracer adsorption in the fault zone.

The upper Paintbrush contact alcove is located in the crystal-poor lower nonlithophysal columnar subzone of the Tiva Canyon Tuff. Two boreholes penetrated the crystal-poor lower nonlithophysal columnar and hackly subzones and the crystal-poor vitric zone of the Tiva Canyon Tuff. Permeability values of the columnar subzone ranged from 0.02×10^{-12} to 2.0×10^{-12} m^2. The arithmetic mean was 0.7×10^{-12} m^2 and the geometric mean was 0.3×10^{-12} m^2. Permeability values of the vitric zone ranged from 0.4×10^{-12} to 57.0×10^{-12} m^2. The arithmetic mean was 16.5×10^{-12} m^2 and the geometric mean was 7.0×10^{-12} m^2. Permeability values of the hackly subzone ranged from 0.1×10^{-12} to 12.0×10^{-12} m^2. The arithmetic mean was 3.7×10^{-12} m^2 and the geometric mean was 2.1×10^{-12} m^2. Water-redistribution pressures of the columnar and hackly subzones and the vitric zone were as low as less than 5.2 kilopascals. The large permeability values of the vitric zone indicated substantial fracturing in the moderately welded to nonwelded vitric zone. Comparison of the upper Paintbrush contact alcove permeability values of the lower nonlithophysal zone to the surface-based permeability values of the lower nonlithophysal zone indicated that the lower nonlithophysal zone may be anisotropic, depending on which of the surface-based permeability values were used for comparison. Comparison of the upper Paintbrush contact alcove permeability values of the vitric zone to the surface-based permeability values (two test intervals) of the vitric zone indicated that the vitric zone is anisotropic and had a vertical to horizontal ratio of about 79:1.

INTRODUCTION

The Yucca Mountain Project is a U.S. Department of Energy (DOE) scientific study to evaluate the potential for geologic disposal of high-level radioactive waste in an unsaturated-zone desert environment. The potential repository site at Yucca Mountain is located about 130 kilometers (km) northwest of Las Vegas, Nevada, near the DOE Nevada Test Site (fig. 1). The U.S. Geological Survey (USGS) has been conducting geologic and hydrologic studies of the potential repository site for the DOE. These studies are to quantify the geologic and hydrologic characteristics of Yucca Mountain and to conceptualize and model gas and liquid flow at the potential repository site.

Single-hole and cross-hole air-injection and tracer testing was conducted in alcoves located in the underground Exploratory Studies Facility (ESF) to quantify the permeability and porosity values of the fractured and unfractured volcanic rocks (tuff). The permeability and porosity of these tuffs control the movement of fluids in Yucca Mountain. Study of these parameters provides an understanding of fluid flow in the unsaturated zone, and the parameters can be used in unsaturated-zone numerical modeling to estimate fluid flux through the mountain. Potential fluid movement in Yucca Mountain includes the transmission of water from the surface to the potential repository horizon and the transmission of gases from the potential repository horizon to the ground surface. Knowledge of the spatial and directional variability of permeability is needed to formulate conceptual models and is required input to flow and transport models that attempt to represent the flow system at Yucca Mountain. This report presents the results from air-injection and tracer testing conducted in the upper Tiva Canyon alcove (UTCA), the Bow Ridge Fault alcove (BRFA), and the upper Paintbrush contact alcove (UPCA) by the USGS from August 1994 through July 1996. The locations of the alcoves and their relations to the potential repository are shown in figure 2.

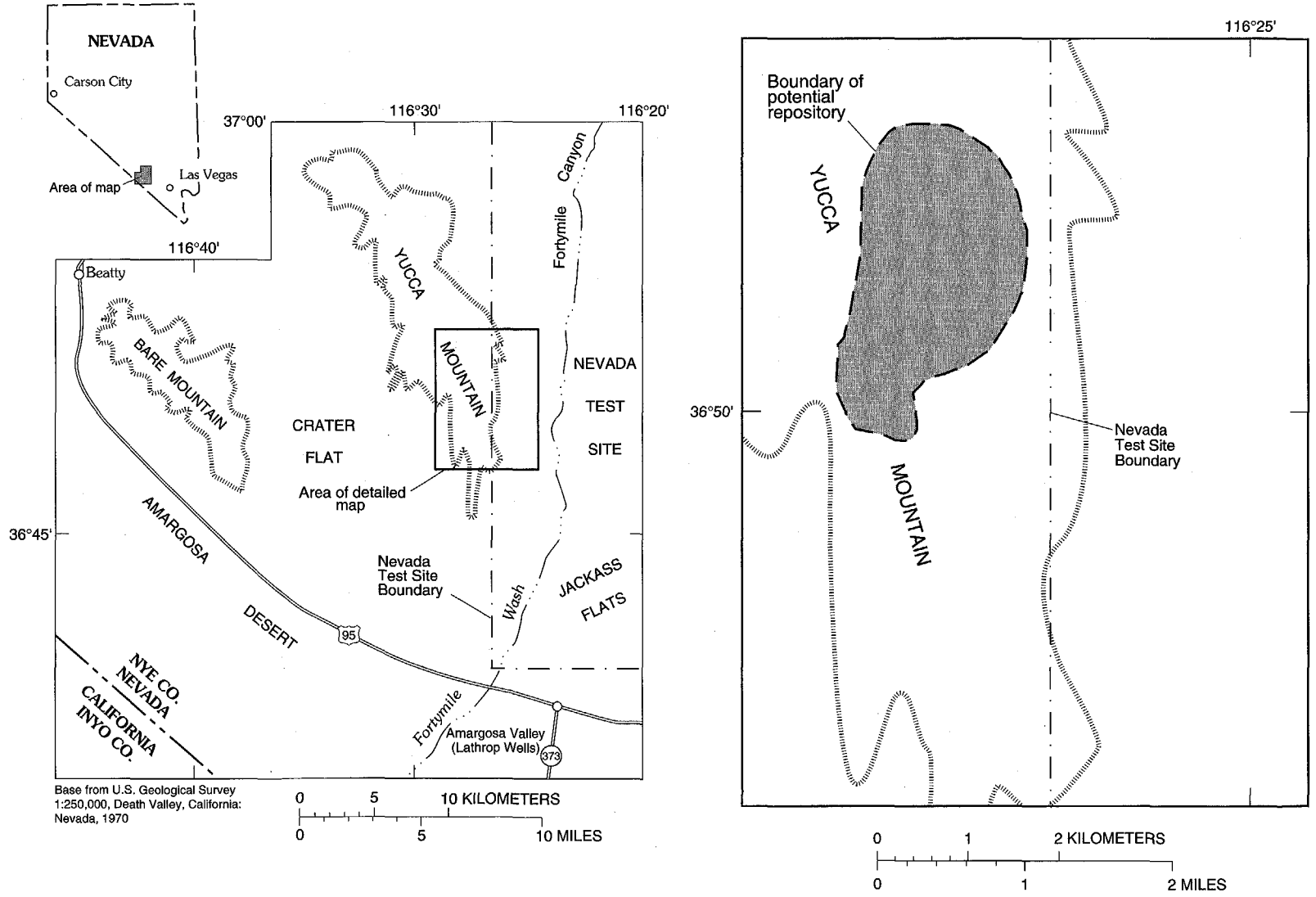

Figure 1. Location of the Nevada Test Site and the potential repository at Yucca Mountain.

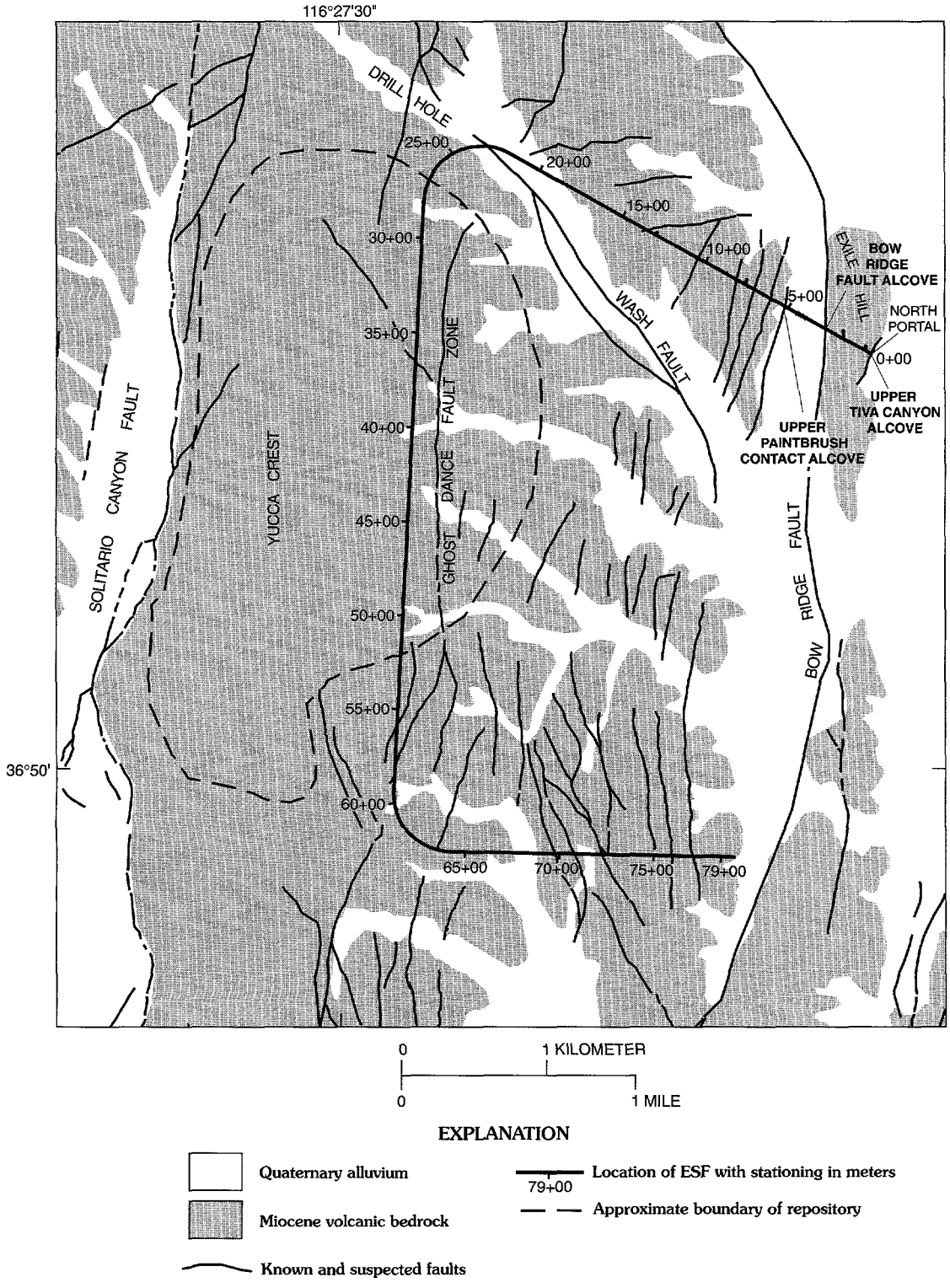

Figure 2. Diagramatic map showing the Exploratory Studies Facility, upper Tiva Canyon, Bow Ridge Fault, and upper Paintbrush contact alcoves.

TEST AND ANALYSIS METHODS

Methods and Analysis for Single-Hole Air-Injection Testing

Single-hole air-injection testing in the unsaturated zone was conducted in horizontal boreholes drilled from the ESF alcoves. The boreholes were 0.1 meter (m) in diameter and 30 m long. A schematic diagram of the single-hole air-injection field testing configuration is shown in figure 3. The field equipment consisted of the downhole-packer system, the air-injection system, and the data-acquisition system. Test intervals were selected from a review of the borehole video and caliper logs. After a test interval was selected, two pneumatic packers were inserted into the borehole straddling the selected test interval, which ranged in length from 1 to 3 m. The packers then were inflated, isolating the test interval from the borehole. After the packers were inflated and the pressure in the test interval had stabilized, compressed air was injected into the isolated test interval through a nylon tube that connected the test interval to an uphole air compressor. Two parts per million (2.0 ppm) sulfur hexafluoride (SF_6) was added to the injection air as a tracer, and the air-injection rate was controlled and monitored by mass-flow controllers. The test-interval absolute pressure and temperature were monitored by a pressure transducer and thermistor mounted between the downhole packers. All data were recorded on a data logger. Air injection was continued until the test-interval pressure reached a steady-state condition. An average test lasted about 10 minutes; however, tests that indicated water redistribution were usually run overnight. Water redistribution was identified as a

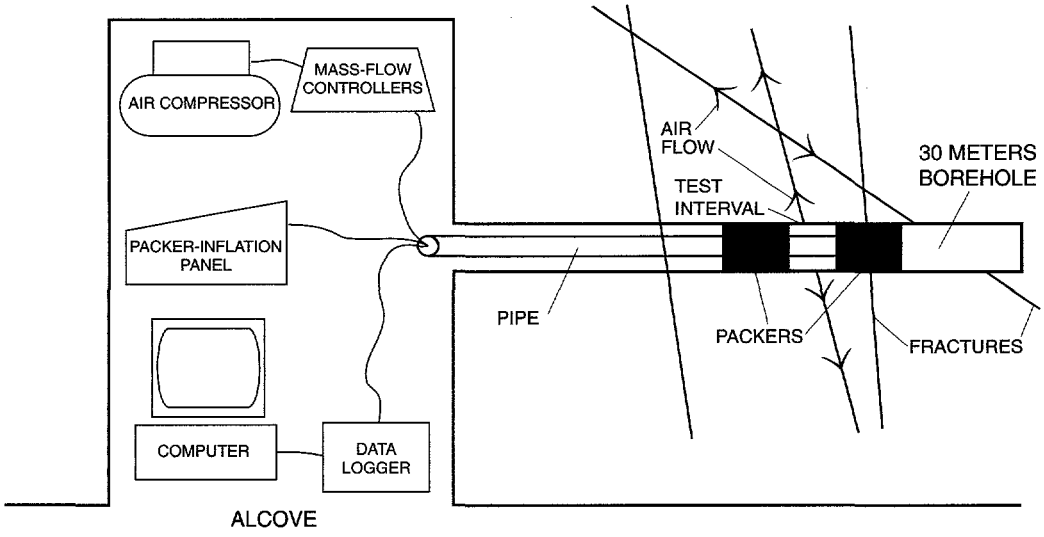

Figure 3. Schematic diagram showing single-hole air-injection testing.

decrease in the air-injection interval pressure with time. Because the air permeability of a rock changes with its water content, a given air permeability also has an associated capillary pressure. Air injection at pressures greater than the rock capillary pressure may result in transient water redistribution. Identification of a break over pressure response, a decrease in pressure with time, indicates near-field water redistribution and represents an upper limit of the near-field capillary pressure (LeCain, 1997). A typical pressure response that indicates water redistribution is presented in figure 4. The pressure peak at 216 kPa and the subsequent decline reflect the transient drainage of water-filled pores or fractures (fig. 4).

To evaluate turbulence and to define the water-redistribution pressure, multiple tests at variable flow rates were performed in each test interval. Field testing began with low flow rates, 10 to 100 standard liters per minute (sLpm), and the flow rate was increased with each additional test until water redistribution was identified, or until the upper limit of the air-injection equipment was reached (about 750 sLpm). When water redistribution was identified, air injection was continued overnight (about 16 hours) to allow the water to redistribute and the pressure to stabilize. For each overnight test, the testing program was reversed the following day and flow rates were decreased during each additional test. Air-injection rates ranged from 10 to 750 sLpm.

Permeability values were calculated for each test by using a modified version of the Hvorslev (1951) steady-state solution. The solution is for elliptical flow when the length of the injection interval is substantially greater than the injection-interval radius. The full derivation of equation 1 is presented in LeCain (1995).

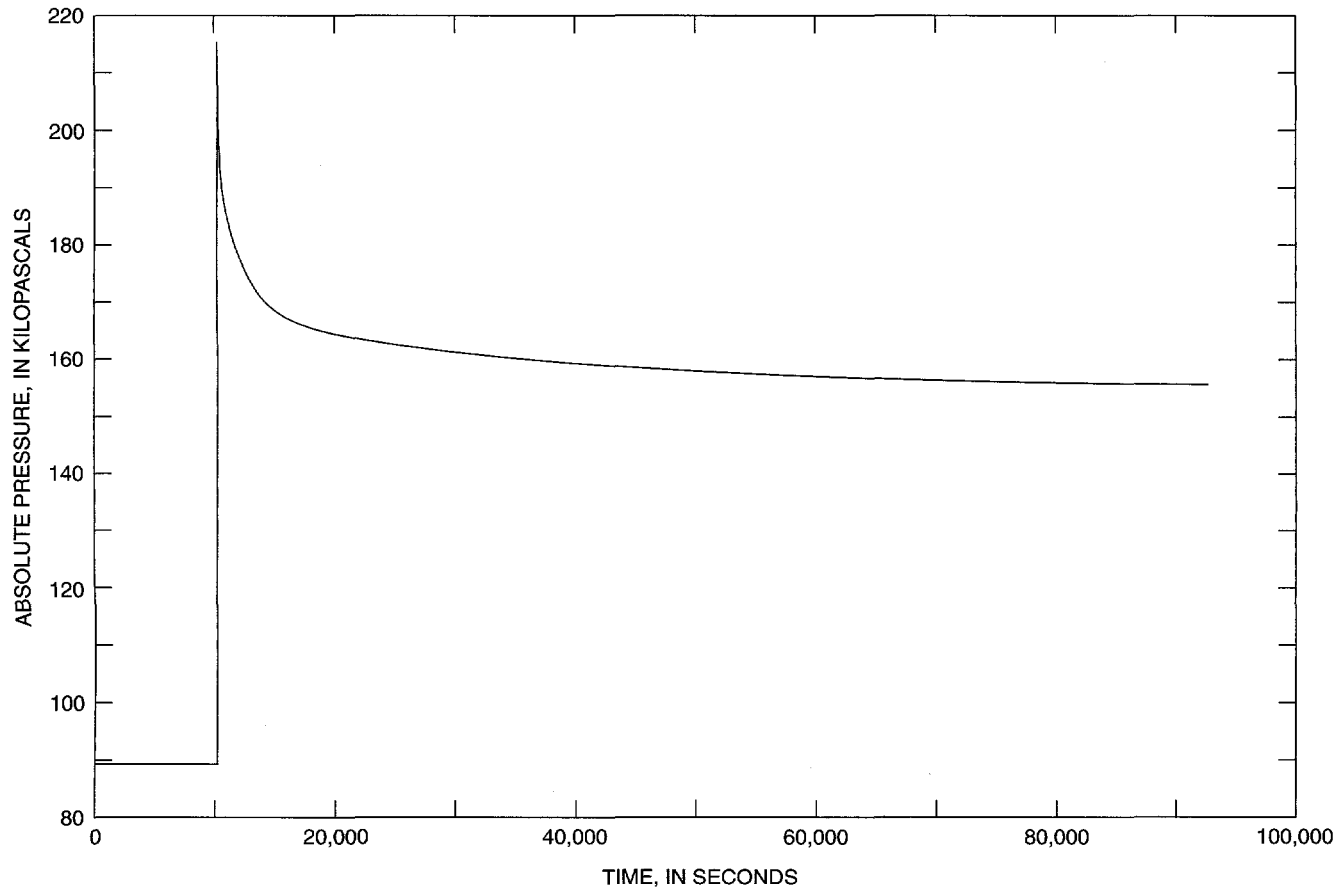

Figure 4. Absolute pressure and times of test 181, upper Paintbrush contact alcove, indicating water redistribution.

$$k = \frac{P_{sc} Q_{sc} \mu ln\left(\frac{L}{2r_w}\sqrt{1+\left(\frac{L}{2r_w}\right)^2}\right)T}{\pi L(P_{ss}^2 - P_0^2)T_{sc}}, \quad (1)$$

where

k = permeability, in meter squared;
P_{sc} = standard pressure, in pascals;
Q_{sc} = flow rate at standard conditions, in cubic meters per second;
μ = dynamic viscosity, in pascal seconds;
L = injection-interval length, in meters;
r_w = borehole radius, in meters;
T = air temperature, in degrees Kelvin;
P_{ss} = pressure at steady state, in pascals;
P_0 = pressure at time zero, in pascals; and
T_{sc} = temperature at standard conditions, in degrees Kelvin.

Because the permeability values may be influenced by the air-injection rate, inertial and turbulent effects must be evaluated. Noman and Archer (1988) credit Forchheimer (1914) for first addressing inertial effects in rock samples. Jacob (1946) addressed turbulence in a pumped well. Forchheimer stated that the differential pressure was a function of the fluid velocity squared. Jacob stated that the head change was a function of the pump rate squared. Ramey (1982), referring to Jacob's work, expanded on the concept with the generalized equation,

$$H_w = BQ + CQ^n, \quad (2)$$

where

H_w = drawdown, in meters;
B = formation-loss term in seconds per meter squared;
Q = flow rate, in cubic meters;
C = well-loss term, units dependent on exponent n; and
n = exponent less than 2.

The first term on the right of equation 2 represents laminar-flow conditions where Darcy's law is valid. The second term represents non-Darcian flow due to turbulence in the borehole or in the fractures or inertial effects in the matrix. The drawdown during Darcian (laminar) flow can be represented by the first term only. During non-Darcian flow, the second term needs to be included. Air-injection testing in fractured rock generally involves a combination of laminar and turbulent fracture flow. Lennox (1966) used a similar equation that included a constant time interval, to account for the nonsteady-state conditions of radial flow, and states that n may be as large as 3.5.

Equation 2 was modified for air-injection testing by substitution of $(P_{ss}^2 - P_0^2)$ for drawdown, and both sides of the equation were divided by the flow rate (Q_{sc}) to give equation 3,

$$\frac{(P_{ss}^2 - P_0^2)}{Q_{sc}} = CQ_{sc}^{n-1} + B, \quad (3)$$

where

P^2_{ss} = steady-state pressure squared, in pascals squared; and
P^2_0 = pressure squared at time zero, in pascals squared.

Equation 3 indicates that an arithmetic plot of the steady-state $(P^2_{ss} - P^2_0)/Q_{sc}$ values, from multiple flow-rate tests, on the y-axis and the Q_{sc} values on the x-axis gives a y-intercept equal to B when Q_{sc} is zero. As Q approaches zero, Darcy's law is valid; that is, there are no turbulent or inertial effects. Equations 1 and 3 can then be combined in equation 4 to provide a laminar-flow air-injection permeability value that is based on the zero-flow intercept B. The method is similar to the multiple flow-rate tests used to compensate for turbulence in the analysis of fractured-rock petroleum reservoirs (Van Golf-Racht, 1982, p. 318-319),

$$k = \frac{P_{sc}\mu ln\left(\frac{L}{2r_w} + \sqrt{1+\left(\frac{L}{2r_w}\right)^2}\right)T}{\pi LBT_{sc}} \quad (4)$$

During field testing, non-Darcian flow was identified as a decrease in the calculated permeability values with increasing flow rates. A check was performed by preparing arithmetic and log-log plots that had the air-injection pressure squared differences $(P^2_{ss} - P^2_0)$ on the y-axis and the flow rate (Q) on the x-axis. Darcian (laminar) flow ($H_w = BQ$) was indicated by a linear arithmetic plot and a log-log plot with a slope of one. A nonlinear arithmetic plot and a log-log plot that had a slope greater than 1 indicated non-Darcian flow. Typical arithmetic and log-log plots are shown in figures 5 and 6. The upward trend of the arithmetic plot (fig. 5) and the 1.2 slope of the log-log

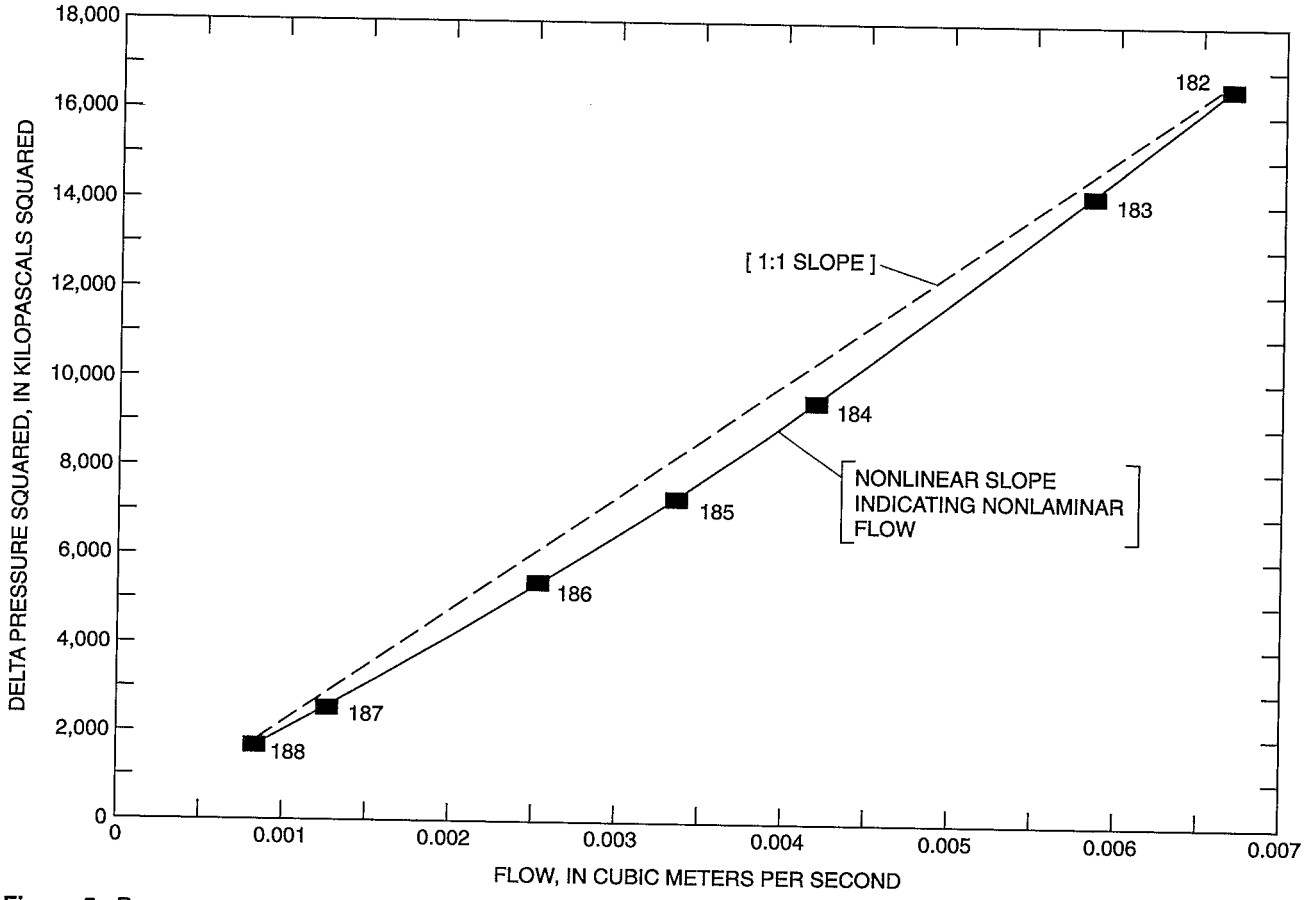

Figure 5. Pressure squared differences and flow rates of tests 182 through 188, upper Paintbrush contact alcove.

plot (fig. 6) indicated non-Darcian flow probably caused by turbulent fracture flow. An arithmetic plot of delta pressure squared difference divided by flow with flow is shown in figure 7. A slope of zero would indicate laminar flow and a positive slope would indicate turbulence. The plot was extrapolated to the y intercept, and the intercept was used in equation 4 to calculate the permeability value.

Methods and Analysis for Cross-Hole Air-Injection Testing

Cross-hole air-injection tests in the unsaturated zone were conducted between horizontal boreholes drilled in the ESF alcoves. The boreholes were 0.1 m in diameter and 30 m long. Cross-hole testing consisted of injecting air into an isolated interval of a borehole (injection borehole) and monitoring the pressure response of isolated monitor intervals in other boreholes (monitor boreholes). The injection borehole was instrumented with the same packer system and support instruments used in the single-hole air-injection testing. The monitor boreholes were instrumented with 8 to 10 packers that separated the monitor boreholes into 8 to 10 pressure monitor intervals. A schematic of the ESF cross-hole air-injection testing is shown in figure 8. The packer lengths ranged from 1.0 to 8.0 m, and the monitor interval lengths ranged from 0.6 to 4.0 m. Each packer was connected to an uphole packer-inflation panel through a dedicated inflation tube. The packer-inflation panel was used to inflate the packers and to monitor the individual packer-inflation pressures. Each monitor interval was connected to an uphole pressure-transducer panel through a dedicated pressure line. Each monitor interval had a dedicated pressure transducer that measured the absolute pressure in the monitor intervals. In addition, the pressure lines could be disconnected from the pressure transducers and used for gas sampling or tracer-gas injection. Air-injection rates ranged from 100 to 400 sLpm and were monitored and controlled by mass-flow controllers. Air was injected until the pressure in the

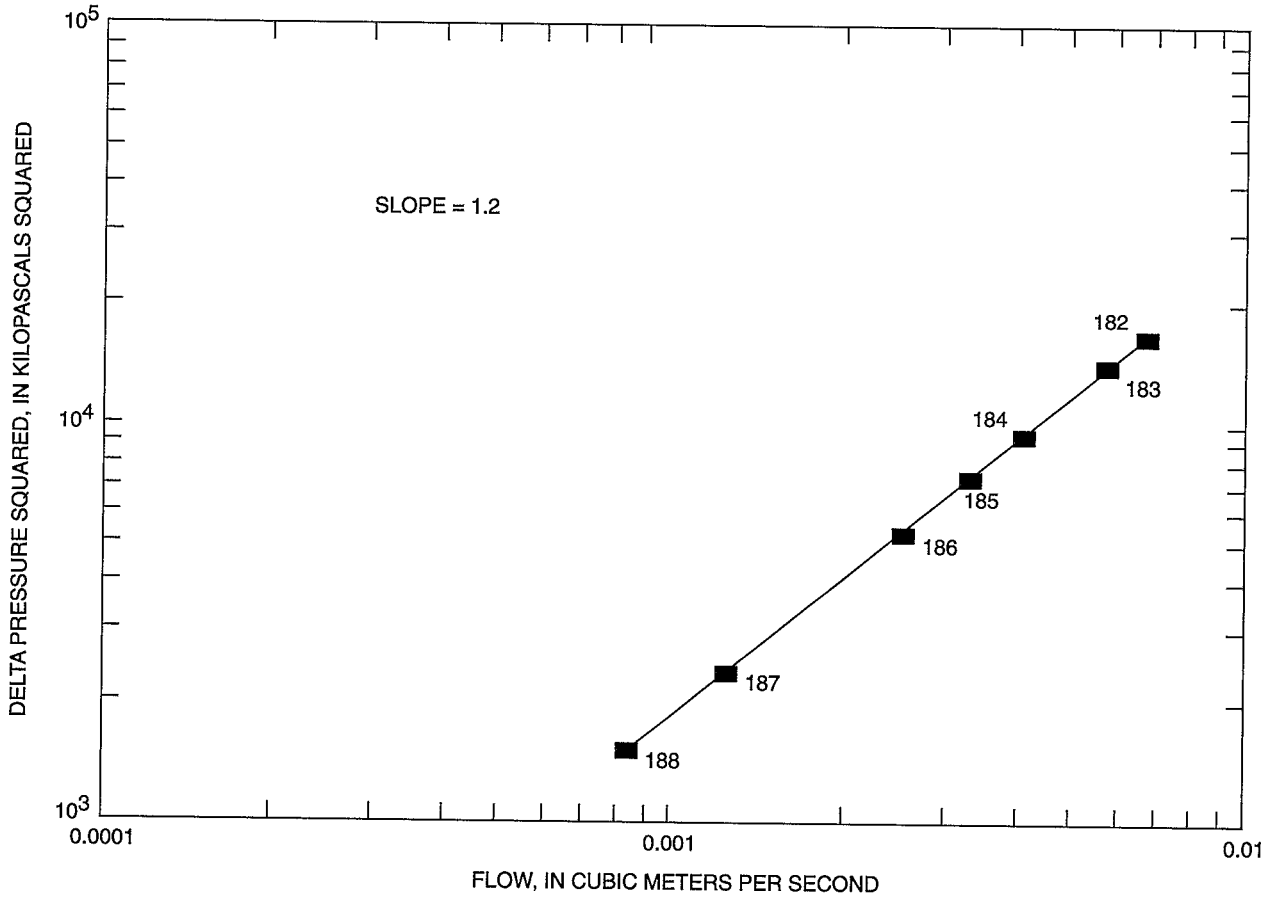

Figure 6. Log-log plot of pressure squared differences and flow rates of tests 182 through 188, upper Paintbrush contact alcove.

injection interval and in the monitor intervals reached steady state.

Type-curve matching was used to analyze the cross-hole air-injection tests. The analysis was based on the assumption of spherical flow geometry and used the complementary error function (Carslaw and Jaeger, 1959) to estimate permeability and porosity values. The full solution is presented in LeCain (1995). The analysis assumed that the injection and the monitoring intervals could be represented as points in a large homogeneous and isotropic system. The solution defines the change, in dimensionless pressure, as:

$$\Delta P_D = \frac{1}{2} erfc\left(\frac{r_D^2}{4t_D}\right)^{\frac{1}{2}}, \qquad (5)$$

where

P_D = change in dimensionless pressure;
$erfc$ = complementary error function;
r_D = dimensionless radius; and
t_D = dimensionless time.

A log-log plot that has the pressure squared differences on the y-axis and time on the x-axis (t=0 at start of the injection test) was overlain on the type curve and a match point was selected. By using the match point variables, the permeability value is

$$k = \frac{TQ_{sc}\mu P_{sc}\Delta P_D}{\Delta P^2 r \pi T_{sc}}, \qquad (6)$$

where

ΔP^2 = pressure squared difference, in pascals squared; and porosity is calculated by

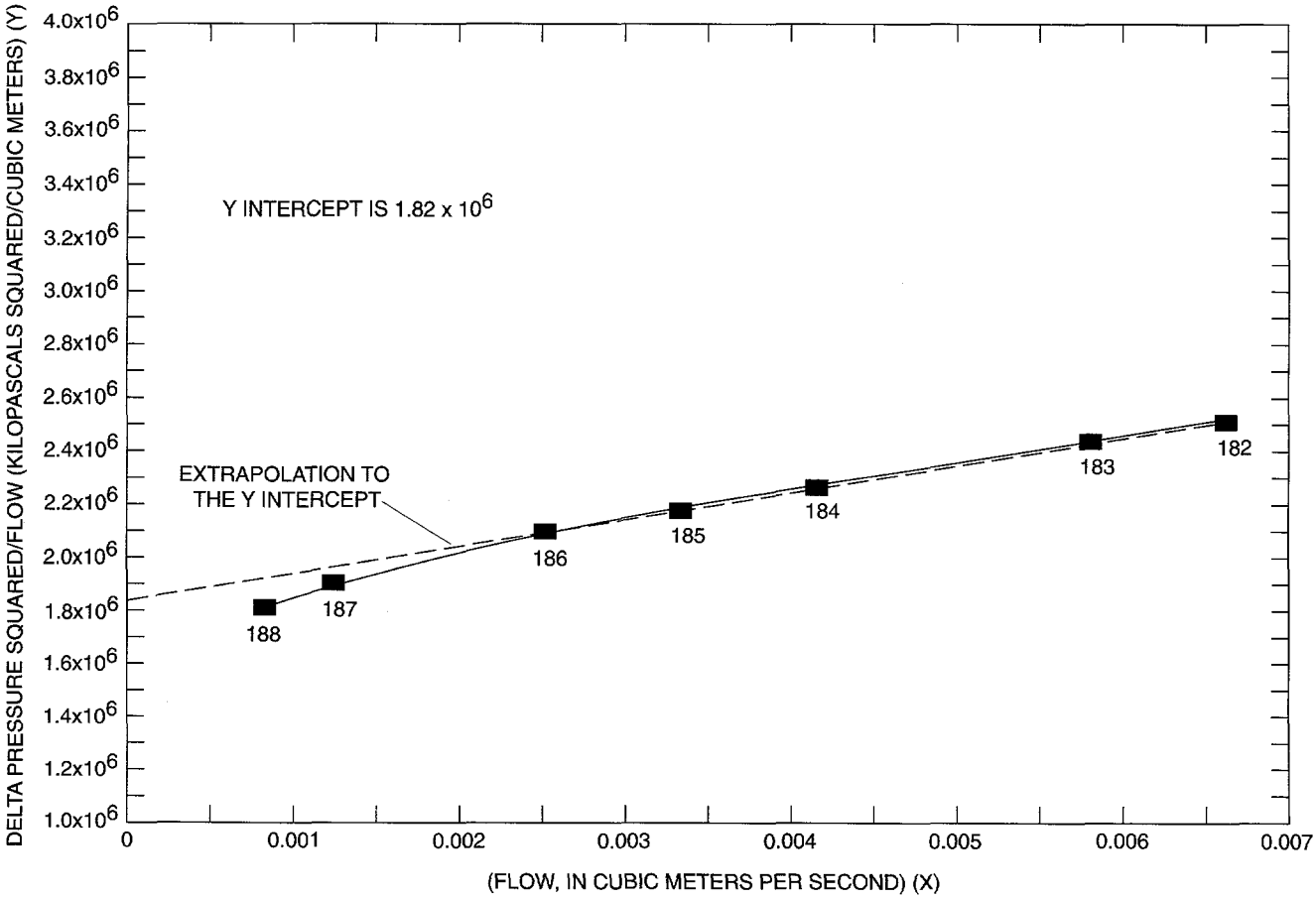

Figure 7. Pressure squared differences divided by the flow rate and flow rates of tests 182 through 188, upper Paintbrush contact alcove, and the y intercept.

$$\phi = \frac{kt\bar{P}}{\left(\frac{t_D}{r_D^2}\right)\mu r^2}, \qquad (7)$$

where

ϕ = porosity, in cubic meter per cubic meter; and
$\bar{P}$ = average pressure, in pascals.

Methods and Analysis for Cross-Hole Tracer Testing

Cross-hole convergent tracer tests were conducted between intervals that had cross-hole air-injection connections. Convergent-tracer testing used the same equipment as cross-hole air-injection testing (fig. 8), except that the air compressor was replaced with a vacuum pump. The test interval, isolated by the single-hole testing packers, was pumped at about 30 sLpm, creating a pneumatic gradient toward the test interval. When the flow system reached steady state, a slug of SF_6 (1 to 10 liters of 10 percent SF_6) was released in a monitor interval of another borehole. The tracer flowed along the pneumatic gradient to the test interval where the tracer concentration was measured. The pumping rate was controlled by mass-flow controllers, the pneumatic gradient was monitored by pressure transducers, and the tracer concentration was measured with an SF_6 leak detector. Tracer concentrations were designed to reach a peak concentration of 35 ppm at the pumped interval.

The tracer concentration from the test interval was plotted with time, and the peak arrival time was identified. The distance between the tracer-release interval and the test interval was divided by the peak arrival time, which resulted in the average tracer velocity,

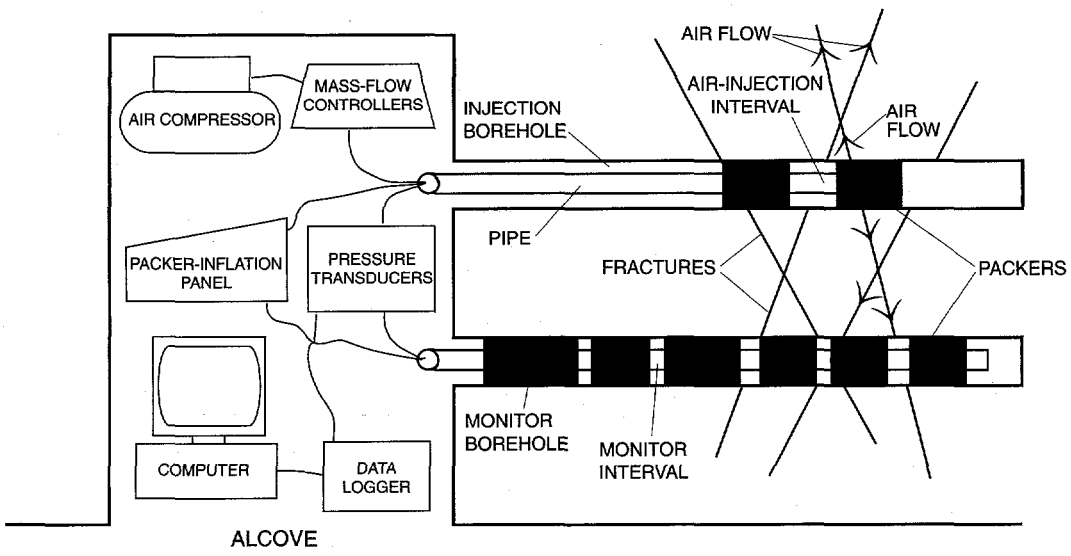

Figure 8. Schematic diagram showing cross-hole air-injection testing.

$$\bar{v} = \frac{d}{t}, \tag{8}$$

where

$\bar{v}$ = average tracer velocity, in meters per second;

t = peak SF_6 arrival time, in seconds; and

d = distance, in meters.

Because the tracer tests were conducted between intervals that had successful cross-hole air-injection tests, the cross-hole permeability values and the tracer-test pneumatic gradient were used to calculate the Darcy velocity,

$$\bar{q} = \frac{k\rho g h}{\mu d}, \tag{9}$$

where

$\bar{q}$ = average Darcy velocity, in meters per second;

r = air density, in kilograms per cubic meter;

g = gravity, in meters per square second; and

h = head difference, in meters of air.

The equation assumes linear flow between the tracer-release interval and the pumped interval. The Darcy velocity is an average velocity because the gradient is an average gradient in a spherical-flow geometry. The true gradient decreases with distance from the pumped interval.

The average tracer velocity can be divided into the Darcy velocity to provide an effective porosity,

$$\phi_{eff} = \frac{\bar{q}}{\bar{v}}, \tag{10}$$

where

ϕ_{eff} = effective porosity.

UPPER TIVA CANYON ALCOVE

Alcove and Borehole Construction

The upper Tiva Canyon alcove (UTCA) (fig. 2) is located 43 m into the ESF measured from the North Portal. The alcove was excavated using controlled drill and blast methods and is about 34 m long and has an average diameter of 5.8 m. The alcove is about perpendicular to the ESF and has a bearing of 21 degrees. Radial boreholes RBT#1, RBT#2, and RBT#3 (fig. 9) were air drilled, producing a 9.6-cm-diameter borehole and 6.4-cm-diameter core. One to 2 ppm SF_6 was added to the drilling air as a tracer for identification of drilling air during future air-chemistry sampling. The boreholes were drilled on the east wall near the end of the alcove. The collars of the boreholes were located about 24 m below the ground surface. The borehole configuration was an expanding triangle that had 3-m sides at the collars and 10-m sides at maximum depth. Borehole RBT#1 was drilled at an angle from vertical of 85.8 degrees and a bearing of 63.2 degrees to a total depth of 30.5 m. Borehole RBT#2 was drilled at an angle from vertical of 86.3 degrees and a bearing of 76.5 degrees to a total depth of 32.1 m. Borehole RBT#3 was drilled at an angle from vertical of 98.4 degrees and a bearing of 69.9 degrees to a total depth of 31.3 m.

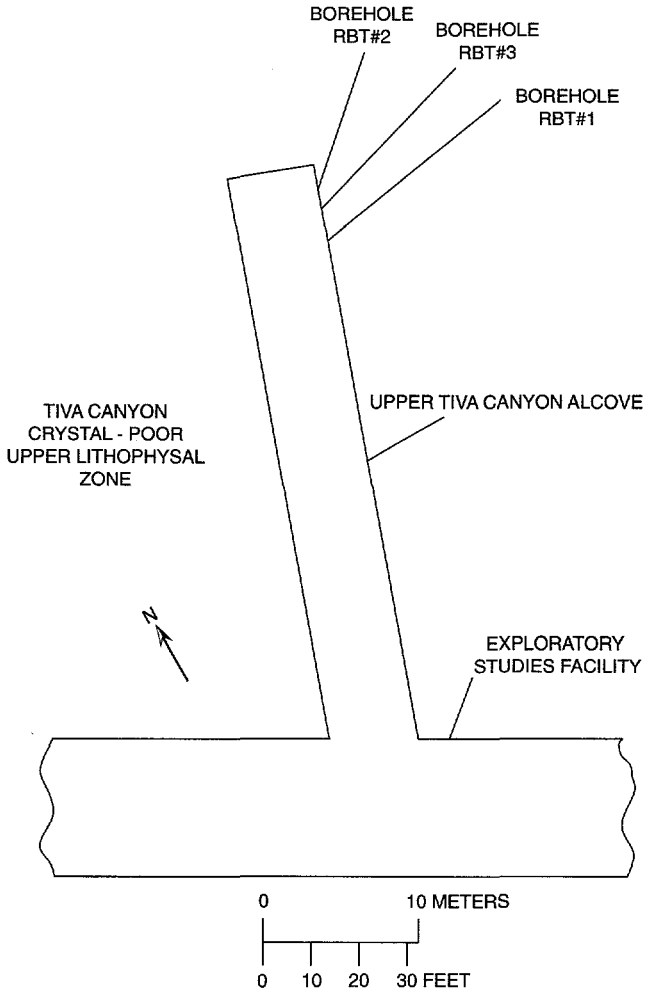

Figure 9. Schematic diagram showing the upper Tiva Canyon alcove and boreholes RBT#1, RBT#2, and RBT#3.

Geology

The UTCA and the three radial boreholes were constructed in the crystal-poor upper lithophysal zone of the Tiva Canyon Tuff (Tpcpul). The tuff is part of the Paintbrush Group of Miocene age and is moderately to densely welded and fractured. Borehole RBT#1 penetrates an ash-flow tuff that is pale reddish brown to pale red, densely welded, and devitrified containing 10 to 20 percent pumice, 2 to 5 percent phenocrysts, and 10 to 12 percent lithophysal cavities. Borehole RBT#2 penetrates an ash-flow tuff that is pale reddish brown, grayish red, and brownish gray; moderately to densely welded; and devitrified, containing 5 to 10 percent pumice, 2 to 10 percent phenocrysts, and 5 percent lithophysal cavities. At a depth of 13.7 m, the phenocryst content increases to 10 percent. Borehole RBT#3 penetrates an ash-flow tuff that is pale red to grayish red, moderately to densely welded, and devitrified containing 3 to 5 percent pumice, decreasing with depth; 3 to 7 percent phenocrysts; and 8 to 15 percent lithophysal cavities (Science Applications International Corporation, written commun., 1995).

Results from Single-Hole Air-Injection Tests

Single-hole air-injection testing was conducted in the UTCA radial boreholes from August through November 1994. The permeability values and water-redistribution pressures from the UTCA single-hole air-injection testing in boreholes RBT#1, RBT#2, and RBT#3 are listed in tables 1 through 3. Test intervals in which water redistribution did not occur are identified with a greater than sign (>) followed by the maximum air-injection pressure measured in the test interval. Test intervals in which water redistribution did occur are identified with a less than sign (<) and the air-injection pressure at which water redistribution first occurred. All the test intervals were in the Tpcpul. The boreholes had very high rugosity due to the lithophysal zones and caving of the borehole walls; therefore, isolation of the test intervals with pneumatic packers was limited and resulted in a limited number of test intervals. Successful air-injection tests were conducted on 25 percent of RBT#1, 55 percent of RBT#2, and 21 percent of RBT#3. Some of the test intervals had no pressure increase during air injection and are identified with an asterisk. The absence of a pressure increase may be due to the packers not seating on the borehole wall and, therefore, leaking; or the permeability of the test interval may be greater

Table 1. Permeability values and water-redistribution pressures from air-injection testing in borehole RBT#1 located in the crystal-poor upper lithophysal zone of the Tiva Canyon Tuff in the upper Tiva Canyon alcove

[NA, not applicable; <, less than; >, greater than; *, no pressure response]

Depth (meters)	Permeability (meter squared $\times 10^{-12}$)	Water-redistribution pressure (kilopascals)
1.5-2.7	*	NA
8.2-9.5	5.5	<37.5
8.8-10.1	11.3	>27.9
8.8-10.1	3.4	<44.0
10.3-11.6	2.3	<22.6
11.2-12.5	*	NA
12.1-13.4	*	NA
18.3-22.0	24.0	>1.4
21.0-22.3	27.0	>2.4
21.3-22.6	3.2	<62.9
26.2-30.6	*	NA

Table 2. Permeability values and water-redistribution pressures from air-injection testing in borehole RBT#2 located in the crystal-poor upper lithophysal zone of the Tiva Canyon Tuff in the upper Tiva Canyon alcove

[NA, not applicable; <, less than; >, greater than; *, no pressure response]

Depth (meters)	Permeability (meter squared $\times 10^{-12}$)	Water-redistribution pressure (kilopascals)
1.2-2.4	47.0	<36.6
2.0-5.0	30.0	>1.3
3.3-4.6	29.0	>1.9
3.4-4.7	26.0	>2.2
3.6-4.9	26.0	>2.3
3.6-4.9	49.0	>2.1
5.0-8.1	76.0	>0.4
6.0-7.3	*	NA
8.5-11.6	*	NA
8.7-11.7	*	NA
11.8-13.1	*	NA
12.1-13.4	*	NA
13.7-14.9	0.8	>130.8
15.1-18.1	28.0	>1.2
16.9-18.1	81.0	>1.2
18.7-20.0	66.0	<11.0
20.6-23.6	30.0	<4.5
24.0-25.3	11.7	<14.1

Table 3. Permeability values and water-redistribution pressures from air-injection testing in borehole RBT#3 located in the crystal-poor upper lithophysal zone of the Tiva Canyon Tuff in the upper Tiva Canyon alcove

[NA, not applicable; <, less than; >, greater than; *, no pressure response]

Depth (meters)	Permeability (meter squared $\times 10^{-12}$)	Water-redistribution pressure (kilopascals)
0.6-1.9	*	NA
1.8-3.1	15.0	>3.8
1.8-3.1	28.0	>2.4
2.1-3.4	27.0	>3.5
2.5-3.8	85.0	>0.8
3.6-4.9	*	NA
4.0-8.5	*	NA
8.6-9.9	0.2	>164.9
10.7-15.2	*	NA
15.5-19.2	23.0	>1.4
20.7-22.0	16.5	<57.1
22.6-27.1	*	NA

than the maximum range of the test equipment (about 100×10^{-12} m^2).

Several test intervals had high permeability values and, therefore, small pressure increases at the maximum flow rate and could not be tested at multiple rates. At small injection pressures, the turbulence or inertial effects should be minimal; therefore, these permeability values were calculated by using equation 1 and are included in this report.

Permeability values from the three boreholes ranged from 0.2×10^{-12} to 85.0×10^{-12} m^2 (tables 1–3); the arithmetic mean was 28.6×10^{-12} m^2 and the geometric mean was 16.0×10^{-12} m^2. Permeability values from tests using different flow rates varied by as much as three times before being corrected for turbulence. Composite histograms of the permeability values from the three radial boreholes and their natural logarithms are shown in figure 10. The histograms are inconclusive because of the small data base, but they indicate that the values were not normally distributed. The apparent lack of a log-normal distribution disagrees with the conclusions of LeCain (1997) that indicated that the distribution of the permeability values in the Tiva Canyon Tuff were log normal. The disagreement may be a result of the limited UTCA borehole testing due to the poor borehole wall condition. The matrix permeability values of core samples from the radial boreholes ranged from 10^{-17} to 10^{-15} m^2 (L. E. Flint, U.S. Geological Survey, written commun., 1996). Comparison of the borehole permeability values with the matrix permeability values indicated that the higher borehole permeability values were due to secondary permeability from fractures.

Water redistribution was not identified in many of the high permeability test intervals because their high permeability limited the maximum air-injection interval differential pressure to a few kilopascals. This is especially true in the UTCA where 28 of the 41 test intervals had maximum air-injection differential pres-

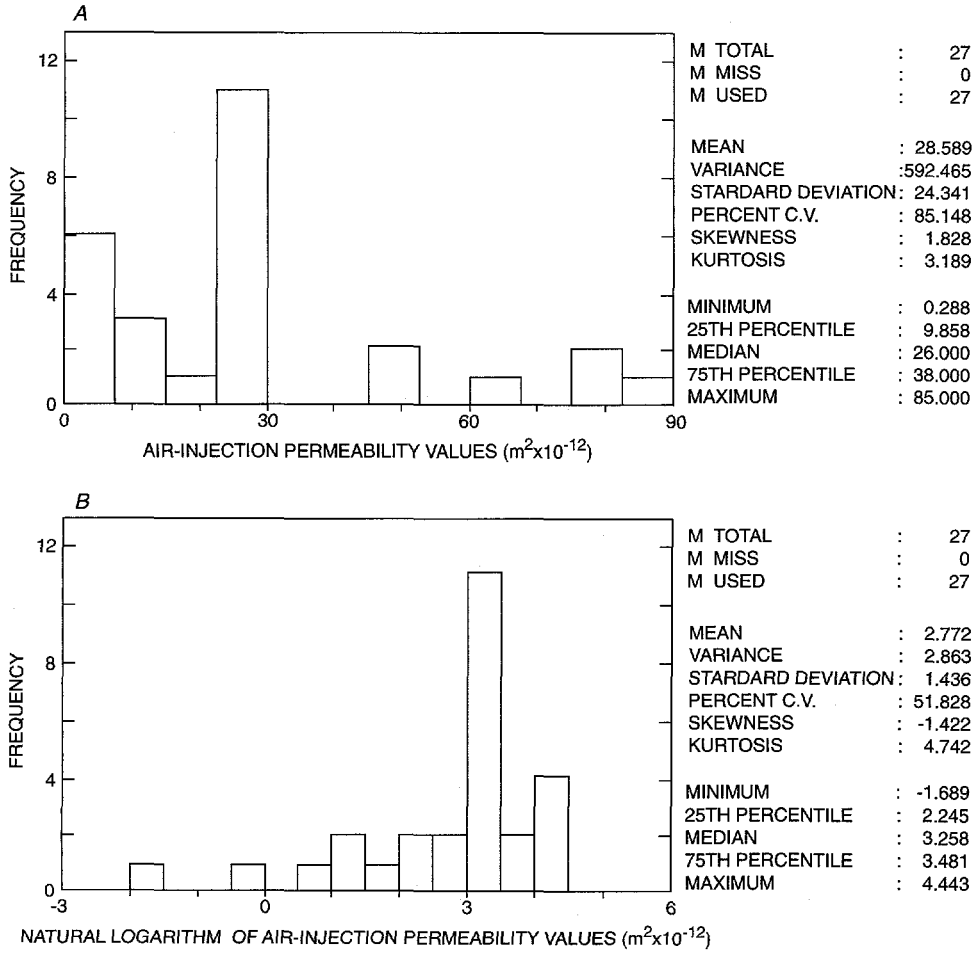

Figure 10. Histograms showing (*A*), air-injection permeability values and (*B*), natural logarithm of air-injection permability values for the boreholes RBT#1, RBT#2, and RBT#3 in the upper Tiva Canyon alcove.

sures of less than 4.5 kPa. Nine test intervals indicated water redistribution. Two test intervals indicated water-redistribution pressures of less than 50 to 100 kPa. Six test intervals indicated water-redistribution pressures of less than 10 to 50 kPa. One test interval indicated a water-redistribution pressure of less than 4.5 kPa.

A statistical summary of the permeability values of the UTCA radial boreholes is presented in table 4. The UTCA Tpcpul permeability values are in the range of the permeability values from the surface-based air-injection testing of the Tiva Canyon crystal-poor lower lithophysal (Tpcpll) and lower nonlithophysal (Tpcpln) zones (LeCain, 1997). Permeability values from vertical boreholes USW SD-12, UE-25 UZ-16, USW NRG-6, and USW NRG-7a in the Tiva Canyon Tuff had arithmetic means that ranged from 7.0×10^{-12} to 26.6×10^{-12} m^2 and geometric means that ranged from 3.4×10^{-12} to 8.7×10^{-12} m^2; the permeability values decreased with increasing depth. The UTCA permeability values were at the high end of the surface-based range. These high values may be associated with increased fracturing or reduced overburden pressure due to the shallow depths in the radial boreholes (about 24 m below the ground surface); however, the surface-based permeability values were for Tpcpll and Tpcpln, making direct comparisons to the Tpcpul of the UTCA questionable.

Fracture network simulations (L.O. Anna, U.S. Geological Survey, written commun., 1996) based on ESF fracture mapping (S.C. Beason and others, Bureau of Reclamation, written commun., 1996) indicated that there are four fracture sets in the Tpcpul. The strike/dip of the four sets (in degrees) are 173/75, 133/83, 240/84, and 164/15. The first three sets are nearly vertical and generally parallel major fault trends, and the fourth set is nearly horizontal. The predominance of nearly vertical fractures indicates that the Tpcpul is anisotropic and has a vertical permeability greater than the horizontal permeability. However, assuming that a permeability value from an air-injection test conducted in a vertical borehole is more representative of the horizontal permeability of the formation, and that a permeability value from an air-injection test conducted in a horizontal borehole is more representative of the vertical permeability of the formation, the similar permeability values derived from air-injection testing in the UTCA horizontal boreholes and from the surface-based vertical boreholes indicate that, at shallow depths, permeability in the Tiva Canyon Tuff is nearly isotropic. An alternate interpretation is that test intervals in the UTCA that had no pressure response indicated permeability values that were greater than the upper range of the equipment (100×10^{-12} m^2); therefore, the true vertical permeability might be greater than the permeability indicated by the UTCA air-injection tests.

Results from Cross-Hole Air-Injection Tests

Cross-hole air-injection testing was conducted between the three radial boreholes in the UTCA from April to July 1995. The cross-hole testing indicated no pneumatic connections between the injection intervals and the monitor intervals. Analytical predictions based on an equivalent porous medium, using the single-hole testing permeability values, indicated that the air-injection rates and pressure-transducer sensitivity would be sufficient to provide cross-hole pressure responses.

Anna (L.O. Anna, U.S. Geological Survey, written commun., 1996) used the ESF fracture-mapping data to develop a stochastic fracture network of the UTCA. An average of 422 fractures were generated, and boreholes RBT#1, RBT#2, and RBT#3 had an average of 20, 22, and 21 single fracture intersec-

Table 4. Statistical summary of the permeability values from air-injection testing in boreholes RBT#1, RBT#2, and RBT#3 located in the crystal-poor upper lithophysal zone of the Tiva Canyon Tuff in the upper Tiva Canyon alcove

[m^2, meter squared]

Borehole	Permeability arithmetic mean ($m^2 \times 10^{-12}$)	Permeability standard deviation ($m^2 \times 10^{-12}$)	Permeability geometric mean ($m^2 \times 10^{-12}$)
RBT#1	11.0	10.4	7.2
RBT#2	38.5	24.0	27.1
RBT#3	27.8	26.9	13.3

tions. An average of 53 fracture networks were connected to at least one borehole. However, the connections between boreholes were sparse and were composed of fractures connected in series. The simulations indicated that few fractures were connected from source to sink, indicating that only a small percentage of the fractures compose the flow path from source to sink. Twenty model realizations were simulated to examine the fracture pneumatic connections between the radial boreholes. Six realizations indicated no fracture pneumatic connections, 4 indicated a single pathway connection from source to sink, and 10 indicated two pathway connections from source to sink.

The fracture modeling indicated that at the scale of the radial boreholes testing (3 to 10 m) cross-hole testing needs to be analyzed using discrete fracture methods and that the absence of any cross-hole pressure responses was due to the combination of a limited number of cross-hole fracture connections and the inability to isolate discrete fractures in the monitor and injection boreholes. The caving and high rugosity of the boreholes severely limited the packer location and spacing and made isolation of individual fractures impossible. The nonideal packer placement resulted in lengths of the monitor intervals of as much as 4 m; therefore, the intervals intersected numerous fractures. The pressure responses in the long monitor intervals represented a composite pressure response of several fractures as opposed to a discrete pressure response representing a single fracture. Even if a fracture did connect a monitor interval and an injection interval, the other fractures would function as constant head boundaries, preventing any pressure increase in the monitor interval.

The absence of cross-hole pneumatic connections prevented cross-hole convergent tracer testing. Without known pneumatic connections it is impossible to select tracer release and sample intervals that provide cross-hole tracer-travel paths.

BOW RIDGE FAULT ALCOVE

Alcove and Borehole Construction

The Bow Ridge Fault alcove (BRFA) is located 168 m into the ESF measured from the North Portal (fig. 2). The alcove was excavated using controlled drill and blast methods. The alcove was constructed at a bearing of 354 degrees. The alcove is about 48 m long and had an initial diameter of 3.7 m. A room for drilling and testing of boreholes was constructed at alcove depths 38 to 48 m. The test room is about 12 m high and 10 m wide. Boreholes for testing the hydrologic properties of faults (HPF) HPF#1 and HPF#2 (fig.11) were air drilled, which produced a 9.6-cm-diameter borehole and 6.4-cm-diameter core. Two ppm SF_6 was added to the drilling air as a tracer for identification of drilling air during future air-chemistry sampling. The two boreholes were drilled on the west wall of the test room. The collars of the boreholes are located about 40 m below the ground surface. The boreholes are horizontal, parallel, and are about 3 m apart. Borehole HPF#1 was drilled at a bearing of 265 degrees to a depth of 26.2 m. Borehole HPF#2 was drilled at a bearing of 265 degrees to a depth of 26.1 m.

Geology

The BRFA is located in the crystal-poor middle nonlithophysal zone (Tpcpmn) of the Tiva Canyon Tuff on the east side (footwall) of the Bow Ridge Fault (fig. 11). The Tiva Canyon Tuff is part of the Paintbrush Group of Miocene age and is densely welded and fractured. The Bureau of Reclamation (BOR) alcove fracture mapping (S.C. Beason and others, Bureau of Reclamation, written commun., 1996) identified the Bow Ridge Fault at 199 m into the ESF (fig. 2), measured from the North Portal, with a strike/dip orientation of 180 degrees/75 degrees. The Bow Ridge Fault is a normal fault that is offset about 128 m. The fault drops the younger, nonwelded, pre-Rainier Mesa bedded tuff #1 (Tmbt1), of Miocene age, down to the Tpcpmn. A cross section of the alcove, fault, geologic contacts, and borehole HPF#1 is shown in figure 12. The fault zone is about 2.7 m wide and contains three breccia zones. The eastern breccia zone, nearest the footwall, is 0.01 to 0.1 m wide and consists of clasts of densely welded fragments of Tiva Canyon Tuff in a matrix of clay and fine sand-sized material from the Tmbt1. The middle breccia zone is about 2.3 m wide and consists of clasts from the Tiva Canyon Tuff and the Tmbt1 in a matrix of clay and fine sand-sized material from the Tmbt1. The western breccia zone, nearest the hanging wall, is about 0.3 m wide and consists of crushed Tmbt1 and minor clasts of the Tiva Canyon Tuff in a matrix of sand-sized

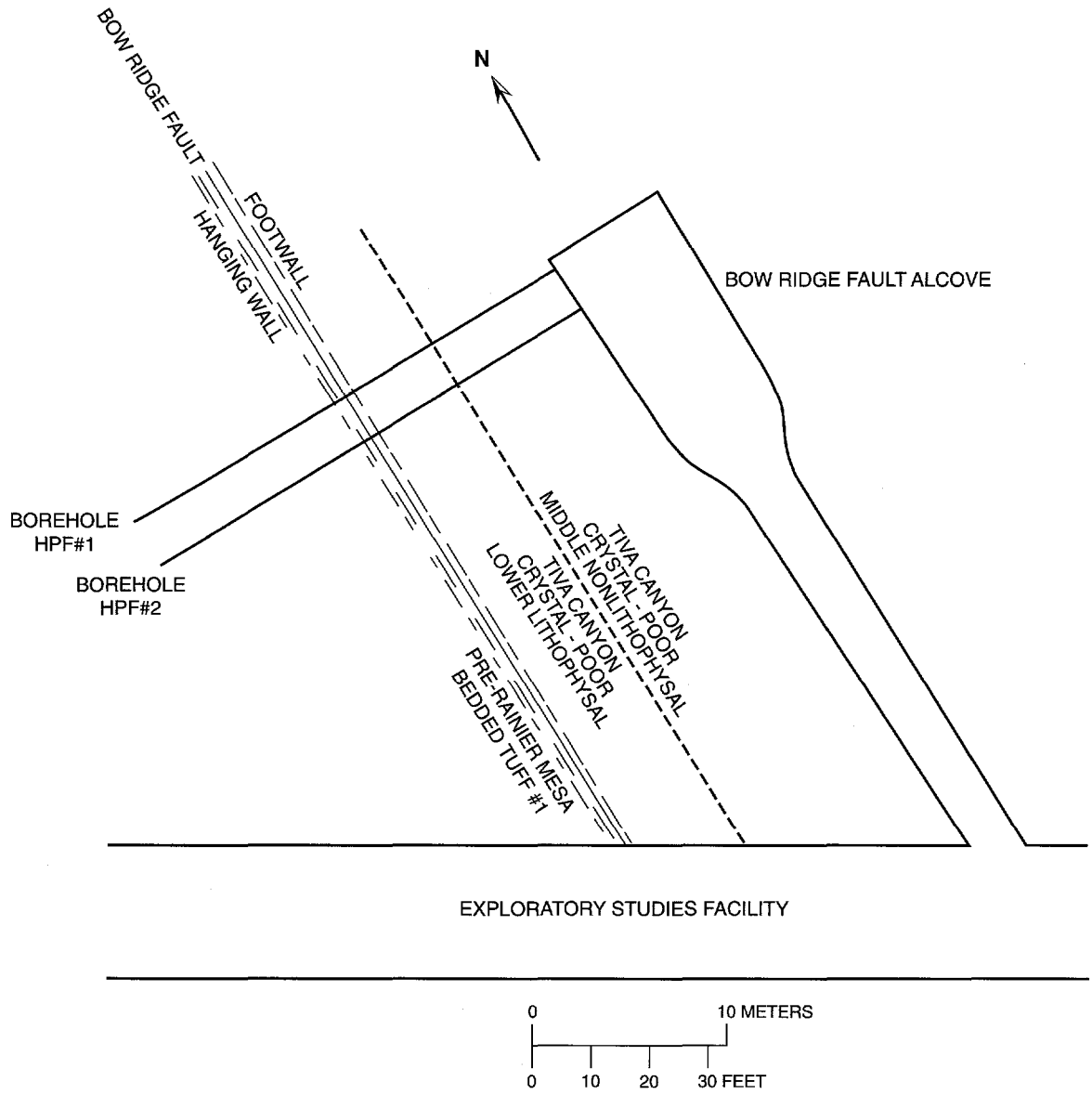

Figure 11. Schematic diagram showing the Bow Ridge Fault alcove and boreholes HPF#1 and HPF#2.

fragments of the Tmbtl (S.C. Beason and others, U.S. Bureau of Reclamation, written commun., 1996).

Borehole HPF#1 was collared in the Tpcpmn. Core logging of borehole HPF#1 by the Sample Management Facility (Science Applications International Corporation, written commun., 1996) identified the first 10.7 m as ash-flow tuff, pale red to grayish red, densely welded and devitrified, containing 5 percent pumice, 5 percent phenocrysts, and 1 percent lithophysal cavities. The contact between the Tpcpmn and the crystal-poor lower lithophysal zone (Tpcpll) of the Tiva Canyon Tuff is at a depth of 10.7 m. From 10.7 to 15.5 m, the lithology changes to an ash-flow tuff that is pale red to grayish red, densely welded and devitrified, containing 3 to 5 percent pumice, 5 percent phenocrysts, and 10 to 15 percent lithophysal cavities. The contact between the Tpcpll and the Bow Ridge Fault zone (figs. 11 and 12) is at a depth of 15.5 m. The fault zone extends from 15.5 to 17.3 m, narrower than identified by the BOR alcove fracture mapping. The contact between the Bow Ridge Fault zone and the Tmbtl is at a depth of 17.3 m. The Tmbtl is a bedded/reworked tuff that is white to very light gray, unconsolidated and vitric, containing 75 percent pumice and 10 percent phenocrysts. Borehole HPF#2 also was collared in the Tpcpmn, and the

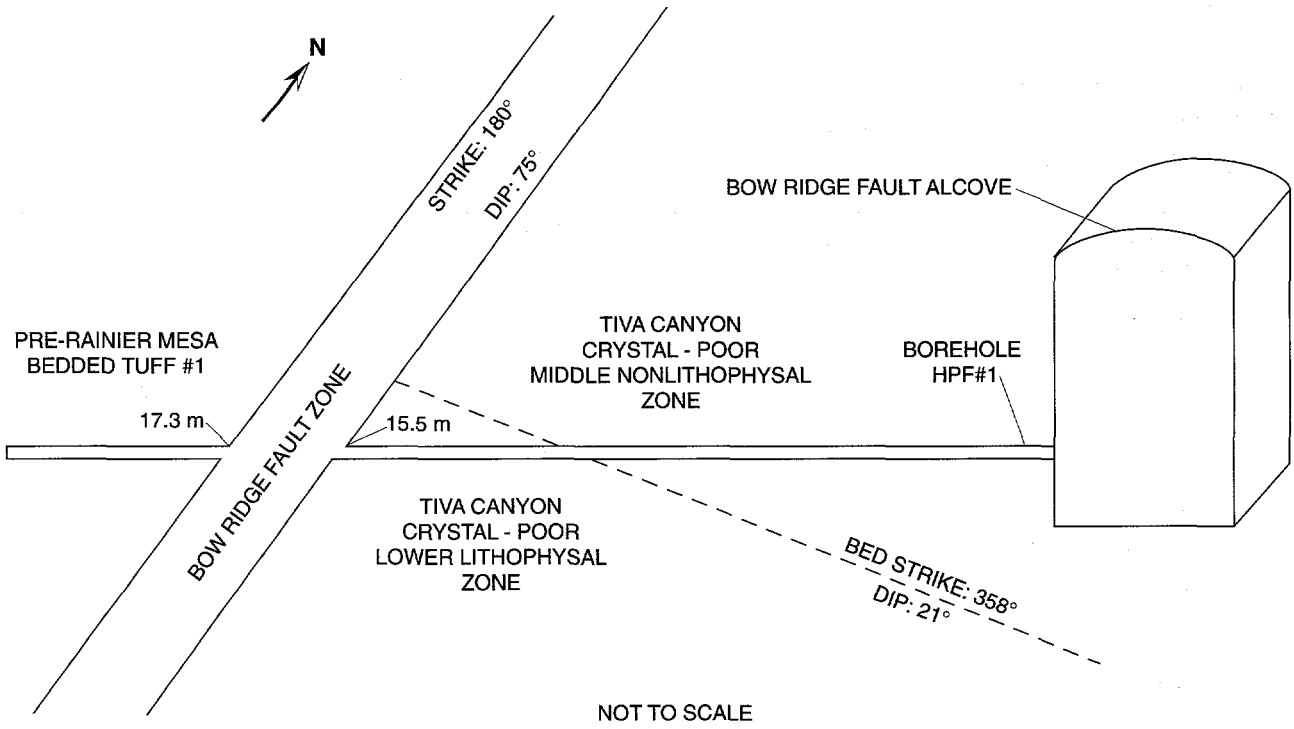

Figure 12. Schematic diagram showing Bow Ridge Fault, Bow Ridge Fault alcove, and borehole HPF#1.

lithology and depth to contacts are almost identical to borehole HPF#1 (Science Applications International Corporation, written commun., 1996).

Results from Single-Hole Air-Injection Tests

Single-hole air-injection testing was conducted in borehole HPF#1 in December 1995 and January 1996. The permeability values, water-redistribution pressures, and geologic zones of the test intervals in borehole HPF#1 are listed in table 5. Test intervals in which water redistribution did not occur are identified with a greater than sign (>) followed by the maximum air-injection pressure measured in the test interval. Test intervals in which water redistribution did occur are identified with a less than sign (<) and the air-injection pressure where water redistribution was first indicated. Testing was conducted in the Tpcpmn and Tpcpll, the Bow Ridge Fault zone, and the Tmbt1. Permeability values of the eight test intervals in the Tpcpmn ranged from 6.0×10^{-12} to 26.4×10^{-12} m^2. Permeability values of the five test intervals in the Tpcpll ranged from 0.6×10^{-12} to 2.0×10^{-12} m^2. Permeability values of the three test intervals in the fault zone ranged from 8.0×10^{-12} to 15.8×10^{-12} m^2. Permeability values of the two Tmbt1 test intervals were 41.3×10^{-12} and 22.0×10^{-12} m^2. Individual test permeability values differed by as much as three times before being corrected for turbulence.

Eleven test intervals in borehole HPF#1 indicated water redistribution (table 5). One test interval had a water-redistribution pressure of less than 50 to 100 kPa. Six test intervals had water-redistribution pressures of less than 10 to 50 kPa. Four test intervals had water-redistribution pressures that were less than 10 kPa, and the lowest was less than 5.6 kPa. Testing in the fault zone and the Tmbt1 did not indicate water redistribution. The absence of water redistribution may be because of high capillary pressures associated with the increased porosity of the nonwelded Tmbt1 or may be because the high permeability of the fault zone and Tmbt1 limited the maximum injection pressures.

A statistical summary of the permeability values for the Tpcpmn and Tpcpll from borehole HPF#1 is in table 6. The Tpcpmn arithmetic mean was 13.9×10^{-12} m^2, and the geometric mean was 12.2×10^{-12} m^2. The Tpcpll arithmetic mean was 1.3×10^{-12} m^2, and the geometric mean was 1.2×10^{-12} m^2. Assuming that the populations were log normally

Table 5. Permeability values, water-redistribution pressures and geologic zones from air-injection testing in borehole HPF#1 located in the Bow Ridge Fault alcove

[m^2, meter squared; <, less than; >, greater than]

Depth (meters)	Permeability ($m^2 \times 10^{-12}$)	Water-redistribution pressure (kilopascals)	Geologic zone
2.2-3.2	8.1	>5.4	Tpcpmn[1]
2.7-4.7	13.7	<9.9	Tpcpmn
3.7-4.7	21.0	>5.9	Tpcpmn
4.6-6.6	21.6	>12.5	Tpcpmn
5.5-6.5	26.4	<28.2	Tpcpmn
7.6-8.6	8.0	<9.5	Tpcpmn
8.6-9.6	6.1	<7.5	Tpcpmn
8.9-9.9	6.0	<5.6	Tpcpmn
10.1-12.1	1.1	<24.2	Tpcpmn-Tpcpll
11.3-12.3	0.9	<63.6	Tpcpll[2]
11.3-12.3	0.6	<20.8	Tpcpll
12.7-14.7	2.0	<35.2	Tpcpll
13.3-14.3	1.7	<12.1	Tpcpll
14.1-15.1	1.5	<13.4	Tpcpll
15.4-17.4	15.8	>8.5	Fault zone[3]
15.8-16.8	8.3	>11.0	Fault zone
15.8-16.8	8.0	>5.1	Fault zone
17.4-19.4	41.3	>4.2	Tmbt1[4]
17.9-18.9	22.0	>11.0	Tmbt1

[1]Tiva Canyon Tuff crystal-poor middle nonlithophysal zone.
[2]Tiva Canyon Tuff crystal-poor lower lithophysal zone.
[3]Bow Ridge Fault zone.
[4]Pre-Rainier Mesa bedded tuff 1.

Table 6. Statistical summary of the permeability values from air-injection testing in borehole HPF#1 located in the Bow Ridge Fault alcove, by geologic zone

[m^2, meter squared]

Geologic zone	Number of test intervals	Permeability		
		Arithmetic mean ($m^2 \times 10^{-12}$)	Standard deviation ($m^2 \times 10^{-12}$)	Geometric mean ($m^2 \times 10^{-12}$)
Tiva Canyon Tuff, crystal-poor middle nonlitho-physal	8	13.9	8.1	12.2
Tiva Canyon Tuff, crystal-poor lower lithophysal	5	1.3	0.6	1.2

distributed, an analysis of variance between the two zones produced a p-value of 0.006, indicating that the means were different. The permeability values for the Tpcpmn in borehole HPF#1 were similar to the permeability values from the surface-based testing of the Tpcpll and Tpcpln (LeCain, 1997). The permeability values for the Tpcpll in borehole HPF#1 were about an order of magnitude smaller than the permeability values from the surface-based testing in the Tpcpll and Tpcpln (LeCain, 1997). The Tpcpll was tested four times during the surface-based testing; permeability values were 0.9, 5.5, 14.0, and 38.0 × 10^{-12} m^2. No surface-based testing was performed on the Tpcpmn.

Assuming that a permeability value from an air-injection test conducted in a vertical borehole is more representative of the horizontal permeability of the formation and a permeability value from an air-injection test conducted in a horizontal borehole is more representative of the vertical permeability of the formation, comparison of the permeability values from the Tpcpmn in borehole HPF#1 with the permeability from the surface-based testing of the Tpcpll and Tpcpln indicated that the permeability of the Tiva Canyon Tuff is isotropic. Comparison of the permeability values from the Tpcpll in borehole HPF#1 with the permeability values from the Tpcpll surface-based testing indicated that the permeability of the Tpcpll is anisotropic with a horizontal to vertical ratio of up to 29:1. The anisotropy is not a function of depth because borehole HPF#1 is located about 40 m below the ground surface and the Tpcpll test intervals from the surface-based testing were located at depths ranging from 30 to 40 m below ground surface. An alternate interpretation is that the indicated anisotropy may be due to the limited spatial distribution and the small surface-based Tpcpll data base.

Results from Cross-Hole Air-Injection Tests

Cross-hole air-injection tests were conducted in the BRFA between boreholes HPF#1 and HPF#2 during May and June 1996. A total of 13 cross-hole tests were conducted using borehole HPF#1 as the injection borehole and borehole HPF#2 as the monitor borehole. Cross-hole testing was conducted in the Tpcpmn, Tpcpll, Bow Ridge Fault zone, and Tmbt1. Several of the cross-hole tests had good pressure responses in as many as three monitor intervals. The permeability and porosity values from cross-hole tests 4, 5, and 6 are listed in table 7. The injection intervals in borehole HPF#1 during tests 1, 2, 3, 7, 9, and 10 did not indicate pneumatic connections to the monitor intervals in borehole HPF#2. The pneumatic responses in tests 8 and 11 indicated a linear flow component; therefore, at the scale of the test, they did not fit the analysis model. The spherical-flow type curve analysis yielded permeability values for the Bow Ridge Fault zone of 27.8 × 10^{-12} and 25.9 × 10^{-12} m^2 and porosities of 0.13 and 0.20; for the Tmbt1, the permeability value was 23.2 × 10^{-12} m^2 and the porosity was 0.27 (table 7). Cross-hole permeability values were within 2 or 3 times those of the single-hole tests.

Table 7. Permeability and porosity values from cross-hole air-injection testing in boreholes HPF#1 and HPF#2 located in the Bow Ridge Fault alcove

[m^2, meter squared; m^3, cubic meter]

Test number	Injection interval in HPF #1	Monitor interval in HPF #2	Permeability ($m^2 \times 10^{-12}$)	Porosity (m^3/m^3)
4	Bow Ridge Fault zone	Bow Ridge Fault zone	27.8	0.13
5	Bow Ridge Fault zone	Bow Ridge Fault zone	25.9	0.20
6	Pre-Rainier Mesa bedded tuff1	Pre-Rainier Mesa bedded tuff1	23.2	0.27

Results from Cross-Hole Tracer Tests

Convergent cross-hole tracer testing, using SF_6, was conducted in the BRFA between boreholes HPF#1 and HPF#2 during June and July 1996. A total of six cross-hole tracer tests were conducted. The analytical results of the BRFA tracer tests are listed in table 8. The tracer velocity is an average velocity based on the peak arrival time. The Darcy velocity is based on the permeability and the pneumatic gradient. Test 1 had problems releasing the slug of tracer; therefore, the results were not usable. During test 4, the tracer slug was released into the Tmbt1. The estimated tracer travel time for test 4 was 110 minutes; the test was halted after 270 minutes when there was no tracer arrival. Tests 5 and 6 were conducted in the Tpcpll and Tpcpmn outside the Bow Ridge Fault zone. Both tests 5 and 6 were successful in measuring the tracer travel times, but the absence of analyzable pneumatic tests makes the analysis of the tracer tests unrealistic.

The effective porosity values from cross-hole tracer tests 2 and 3 were larger than the corresponding porosity values from cross-hole air-injection tests 4 and 5 (table 7). The larger effective porosity values indicated increased tortuosity or adsorption of the tracer. Adsorption testing of SF_6 by Rattray and others (1995) indicated that SF_6 is readily adsorbed onto materials that have a high cation-exchange capacity (clinoptilolite, bedded tuff, and Topopah Spring Tuff). Rattray reported that the Tiva Canyon Tuff had a low cation-exchange capacity and did not appreciably adsorb SF_6; however, the clay and sand-size Tmbt1 material, which makes up the matrix of the fault zone breccia, has the potential to retard the tracer. The relatively large effective porosity values in the fault zone may be due to tracer adsorption. Adsorption also may explain the loss of all tracer during cross-hole tracer test 4, which was conducted in the Tmbt1, and the identical first arrival times but different peak arrival times of tracer tests 2 and 3. The tracer released in test 2 may have occupied adsorption sites; therefore, the tracer gas released in tracer test 3 had less adsorption and a faster average velocity.

UPPER PAINTBRUSH CONTACT ALCOVE

Alcove and Borehole Construction

The upper Paintbrush contact alcove (UPCA) is located 754 m into the ESF, measured from the North Portal (figs. 2 and 13). The alcove was excavated using a mechanical miner. The alcove was constructed at a heading of due north (bearing 0 degrees) to a depth of about 22 m and had a diameter of about 3.7 m. At a depth of 22 m, the alcove heading was changed to 17 degrees and the alcove was excavated an additional 14 m and had a diameter of about 5 m. Radial boreholes RBT#1 and RBT#4 (fig. 13) were air drilled producing 9.6-cm-diameter boreholes and 6.4-cm-diameter cores. Two ppm SF_6 was added to the drilling air as a tracer for identification of drilling air during future air chemistry sampling. The boreholes were collared at about 101 m below the ground surface. Borehole RBT#1 was horizontally drilled, on the west wall, at a heading of 287 degrees to a depth of 30.7 m. Borehole RBT#4 was horizontally drilled, on the east wall, at a heading of 107 degrees to a depth of 30.5 m.

Table 8. Test results from cross-hole tracer testing in boreholes HPF#1 and HPF#2 located in the Bow Ridge Fault alcove

[m/s, meter per second]

Test number	Pumped interval HPF#1	Release interval HPF#2	First arrival (minutes)	Peak arrival (minutes)	Tracer velocity ($\times 10^{-4}$ m/s)	Darcy velocity ($\times 10^{-4}$ m/s)	Effective porosity
2	Bow Ridge Fault zone	Bow Ridge Fault zone	16	80	6.5	3.1-3.4	0.48-0.52
3	Bow Ridge Fault zone	Bow Ridge Fault zone	16	36	14.4	3.1-3.4	0.22-0.24

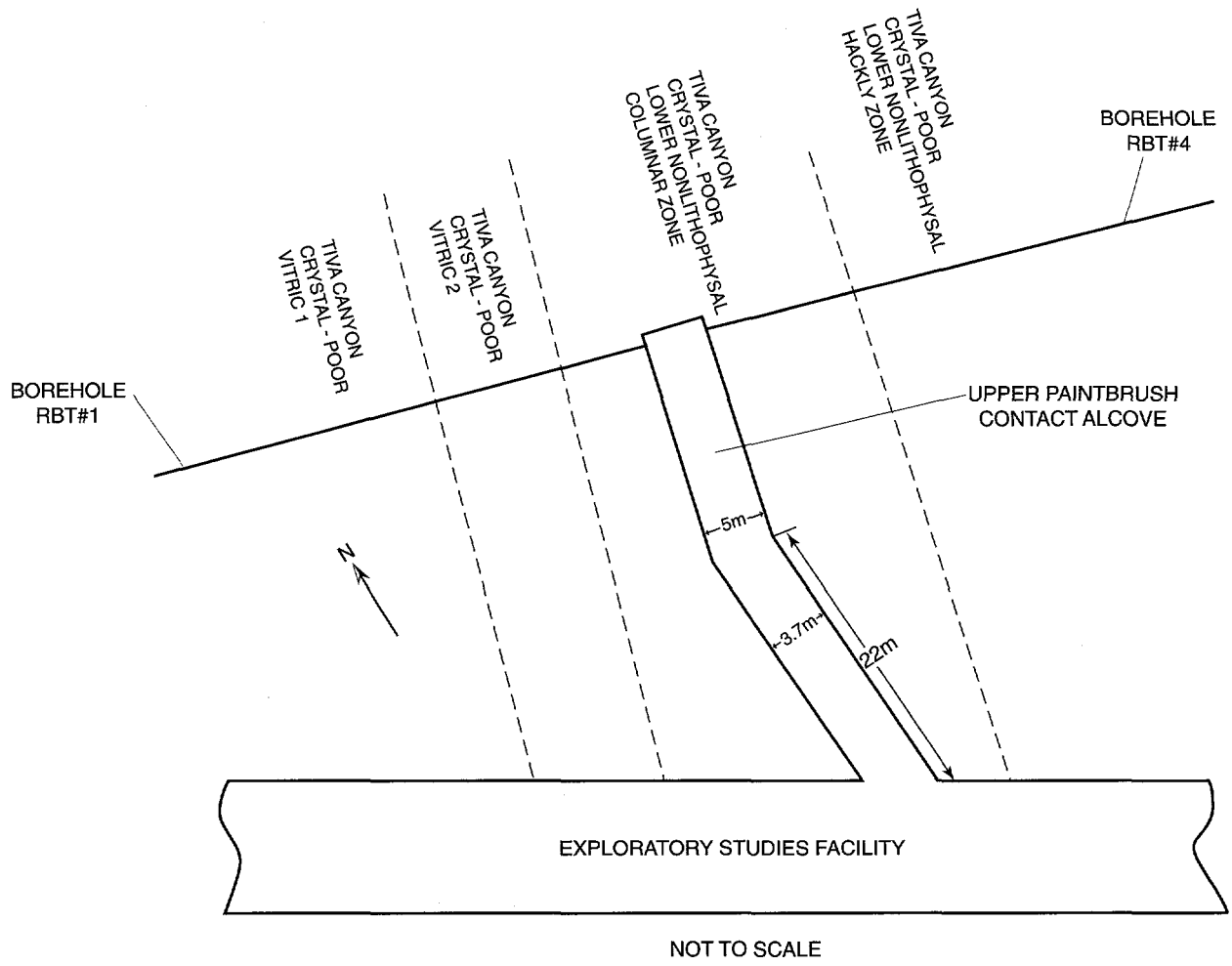

Figure 13. Schematic diagram showing upper Painbrush contact alcove and boreholes RBT#1 and RBT#4.

Geology

The UPCA is located in the moderately welded, crystal-poor, lower nonlithophysal columnar subzone (Tpcplnc) of the Tiva Canyon Tuff. The Tiva Canyon Tuff is part of the Paintbrush Group of Miocene age. Borehole RBT#1 was collared in the Tpcplnc and the first 4.2 m is ash-flow tuff that is pale red to light brown and devitrified, containing 8 to 15 percent pumice and 3 to 5 percent phenocrysts. The welding decreases and the porosity increases with depth. At a depth of 4.2 m, borehole RBT#1 intersects the crystal-poor vitric subzone 2 (Tpcpv2) of the Tiva Canyon Tuff, and at a depth of 12.2 m, the borehole intersects the crystal poor vitric subzone 1 (Tpcpv1) of the Tiva Canyon Tuff. The Tpcpv1 and the Tpcpv2 are pyroclastic-flow deposits that are grayish orange to dark gray and vitric, containing 3 to 12 percent pumice and 3 to 6 percent phenocrysts in an argillically altered matrix. Welding decreases with depth, becoming nonwelded at the Tpcpv2/Tpcpv1 boundary. Borehole RBT#4 was collared in the Tpcplnc. The Tpcplnc is an ash-flow tuff that is grayish pink and devitrified, containing 3 to 15 percent pumice and 3 to 5 percent phenocrysts. Welding increases with depth. At a depth of about 9 m, borehole RBT#4 intersects the crystal-poor lower nonlithophysal hackly subzone (Tpcplnh) of the Tiva Canyon Tuff, and the fracture pattern changes from columnar to hackly (Science Applications International Corporation, written commun., 1995).

Results from Single-Hole Air-Injection Tests

Single-hole air-injection testing was conducted in boreholes RBT#1 and RBT#4 in the UPCA from April through June 1996. The permeability values, water-redistribution pressures, and geologic zones of the test intervals in boreholes RBT#1 and RBT#4 are listed in tables 9 and 10. Test intervals in which water redistribution did not occur are identified with a greater than sign (>) followed by the maximum air-injection pressure measured in the test interval. Test intervals in which water-redistribution did occur are identified with a less than sign (<) and the air-injection pressure where water redistribution was first indicated. The geologic zones tested were the Tpcplnc, Tpcv1, Tpcpv2, and Tpcplnh. All test-interval lengths were 1 m, except for the bottom-hole tests which had lengths of 3.2 and 5.0 m. Permeability values for the Tpcplnc ranged from 0.02×10^{-12} to 2.0×10^{-12} m^2 and had an arithmetic mean of 0.7×10^{-12} m^2 and a geometric mean of 0.3×10^{-12} m^2. Permeability values for the Tpcpv1 and Tpcpv2 ranged from 0.4×10^{-12} to 57.0×10^{-12} m^2 and had an arithmetic mean of 16.5×10^{-12} m^2 and a geometric mean of 7.0×10^{-12} m^2. Permeability values for the Tpcplnh ranged from 0.1×10^{-12} to 12.0×10^{-12} m^2 and had an arithmetic mean of 3.7×10^{-12} m^2 and a geometric mean of 2.1×10^{-12} m^2. Individual test permeability values differed by as much as three times before correcting for turbulence. The relatively large permeability values of the Tpcpv subzones compared to the Tpcpln subzones indicated fracturing in the less welded Tpcpv subzones.

Twenty-two test intervals in the UPCA indicated water redistribution. Two of the test intervals indicated water-redistribution pressures of less than 50 to 100 kPa. Fourteen of the test intervals indicated water-redistribution pressures of less than 10 to 50 kPa. Six test intervals indicated water-redistribution pressures of less than 10 kPa, and the lowest was less than 5.2 kPa.

A statistical summary, by geologic zone, of the permeability values from the UPCA and the permeability values from the surface-based testing program (LeCain, 1997) is listed in table 11. An analysis of variance between the two data bases was performed by using the natural logs of the permeability values. The results were contradictory and inconclusive, probably because of the limited data base. In summary, the data indicated that the permeability values from the Tpcplnh and Tpcplnc at the UPCA were generally equal to or smaller than the permeability values from the surface-based testing, and the permeability values from the Tpcpv at the UPCA were larger than the permeability values from the surface-based testing. Assuming that a permeability value from an air-injection test conducted in a vertical borehole is more representative of the horizontal permeability of the formation, and that a permeability value from an air-injection test conducted in a horizontal borehole is more representative of the vertical permeability of the formation, the following interpretations are possible. The permeability of the Tpcplnh may be anisotropic and have a horizontal to vertical ratio of about 8:1, depending on which of the surface-based permeability values are being used for comparison. The permeability of the Tpcplnc may be anisotropic and have a horizontal to vertical ratio of as much as 37:1, depending on which of the surface-based permeability values are used for comparison. Despite the predominance of vertical fracturing in the Tiva Canyon Tuff (S.C. Beason, U.S. Bureau of Reclamation, written commun., 1996), results do not indicate that the vertical permeability of the Tpcpln is greater than its horizontal permeability. The small surface-based data base (two test intervals) for the Tpcpv indicated that the permeability of the Tpcpv is anisotropic and has a vertical to horizontal ratio of about 79:1.

Comparison of the permeability values of the UPCA with the permeability values of the surface-based testing program needs to account for the fact that the surface-based testing indicated statistically significant differences between the four surface-based boreholes (LeCain, 1997). Therefore, the fact that permeability values from a single ESF alcove agreed with some of the surface-based permeability values and not others is not surprising. Differences in test interval depths may account for some of the variance. The UPCA boreholes are located about 101 m below the ground surface, whereas the surface-based test intervals were located at depths that ranged from 11.7 to 70 m; the permeability values decreased with increasing depth (LeCain, 1997). The larger permeability values from the surface-based testing of the Tpcplnh and Tpcplnc may be due to stress relief fracturing or opening of existing fractures due to small overburden pressures.

Table 9. Permeability values, water-redistribution pressures, and geologic zones from air-injection testing in borehole RBT#1 located in the upper Paintbrush contact alcove

[m^2, meter squared; <, less than; >, greater than]

Depth (meters)	Permeability ($m^2 \times 10^{-12}$)	Water-redistribution pressure (kilopascals)	Geologic zone
1.9-2.9	1.6	<8.8	Tpcplnc
3.7-4.7	0.2	<8.4	Tpcplnc
5.5-6.5	9.3	<8.9	Tpcpv2[2]
7.4-8.4	41.1	<6.6	Tpcpv2
13.8-14.8	57.0	>11.2	Tpcpv1[3]
14.7-15.7	33.9	<11.7	Tpcpv1
16.5-17.5	15.0	<5.2	Tpcpv1
18.4-19.4	0.4	<24.1	Tpcpv1
20.3-21.3	13.0	>12.7	Tpcpv1
22.0-23.0	1.1	>88.9	Tpcpv1
23.8-24.8	7.7	>21.1	Tpcpv1
25.7-26.7	0.9	<95.2	Tpcpv1
27.5-28.5	1.9	<77.6	Tpcpv1
27.5-30.7	17.0	<11.6	Tpcpv1

[1]Tiva Canyon Tuff crystal-poor lower nonlithophysal columnar subzone.
[2]Tiva Canyon Tuff crystal-poor vitric subzone 2.
[3]Tiva Canyon Tuff crystal-poor vitric subzone 1.

Table 10. Permeability values, water-redistribution pressures, and geologic zones from air-injection testing in borehole RBT#4 located in the upper Paintbrush contact alcove

[m^2, meter squared; <, less than; >, greater than]

Depth (meters)	Permeability ($m^2 \times 10^{-12}$)	Water-redistribution pressure (kilopascals)	Geologic zone
1.9-2.9	2.0	>110.9	Tpcplnc[1]
3.7-4.7	0.02	>99.7	Tpcplnc
5.5-6.5	0.06	<73.6	Tpcplnc
7.4-8.4	0.4	<77.6	Tpcplnc
9.2-10.2	0.4	<66.6	Tpcplnh[2]
11.0-12.0	4.7	<51.7	Tpcplnh
12.9-13.9	1.7	<7.5	Tpcplnh
14.7-15.7	0.1	<44.5	Tpcplnh
16.5-17.5	6.2	<22.2	Tpcplnh
18.4-19.4	3.1	<16.2	Tpcplnh
20.2-21.2	12.0	<14.1	Tpcplnh
22.0-23.0	6.2	<34.7	Tpcplnh
23.9-24.9	1.0	<37.2	Tpcplnh
25.5-26.5	2.3	<43.8	Tpcplnh
25.5-30.5	2.9	>43.5	Tpcplnh

[1]Tiva Canyon Tuff crystal-poor lower nonlithophysal columnar subzone.
[2]Tiva Canyon Tuff crystal-poor lower nonlithophysal hackly subzone.

Table 11. Statistical summary of the permeability values for the upper Paintbrush contact alcove and for the surface-based testing program, by geologic zone

[Permeability values in meter squared × 10^{-12}; mean, arithmetic mean; #, number of test intervals; GM, geometric mean; surface-based permeability values from LeCain (1997)]

		Surface based			
	UPCA	UE-25 UZ-16	USW SD-12	USW NRG-6	USW NRG-7a
Geologic zone	mean range (#) GM	mean range (#) GM	mean range (#) GM	mean range (#) GM	mean range (#) GM
Tpcplnh[1]	3.7	--	1.7	28.0	--
	0.1-12.0	--	--	--	--
	(11)	--	(1)	(1)	--
	2.1	--	1.7	28.0	--
Tpcplnc[2]	0.7	15.0	2.9	1.3	25.7
	0.02-2.0	--	0.8-5.9	0.3-2.3	11.0-41.0
	(6)	(1)	(3)	(2)	(2)
	0.3	15.0	2.1	0.8	21.2
Tpcpv1 and 2[3]	16.5	--	--	--	0.2
	0.4-57.0	--	--	--	0.1-0.3
	(12)	--	--	--	(2)
	7.0	--	--	--	0.2

[1]Tiva Canyon crystal-poor lower nonlithophysal hackly subzone.
[2]Tiva Canyon crystal-poor lower nonlithophysal columnar subzone.
[3]Tiva Canyon crystal-poor vitric subzones 1 and 2.

SUMMARY

Single-hole and cross-hole air-injection and tracer testing was conducted in alcoves located in the Exploratory Studies Facility at Yucca Mountain, Nevada. The objectives of these tests were to quantify the permeability and porosity values of the volcanic rocks (tuff). This report presents the results from air-injection and tracer testing conducted in the upper Tiva Canyon alcove (UTCA), the Bow Ridge Fault alcove (BRFA), and the upper Paintbrush contact alcove (UPCA) during August 1994 through July 1996.

The UTCA is located in the moderately to densely welded crystal-poor upper lithophysal zone (Tpcpul) of the Tiva Canyon Tuff, part of the Paintbrush Group of Miocene age. Three boreholes were drilled into the Tpcpul, and single-hole and cross-hole air-injection testing was conducted. The single-hole permeability values ranged from 0.2×10^{-12} to 85.0×10^{-12} m^2; the arithmetic mean was 28.6×10^{-12} m^2, and the geometric mean was 16.0×10^{-12} m^2.

Nine test intervals indicated water redistribution. Two test intervals indicated water-redistribution pressures of less than 50 to 100 kPa. Six test intervals indicated water-redistribution pressures of less than 10 to 50 kPa. One test interval indicated a water-redistribution pressure of less than 4.5 kPa.

Comparison of the single-hole permeability values with the matrix permeability values (10^{-17} to 10^{-15} m^2 from L.E. Flint, U.S. Geological Survey, written commun., 1996) indicated that the larger single-hole permeability values were due to secondary fracture permeability. The UTCA Tpcpul permeability values were in the range of the permeability values from the surface-based testing of the Tpcpln and Tpcpll (LeCain, 1997). The similar permeability values indicated that, at shallow depths, the Tiva Canyon Tuff is nearly isotropic. However, an alternate

interpretation is that the test intervals in the UTCA that had no pressure response indicated permeability values that were greater than the upper range of the equipment (100×10^{-12} m^2); therefore, the true vertical permeability might be greater than the permeability indicated by the UTCA air-injection tests.

Cross-hole air-injection testing in the UTCA failed to locate any pneumatic connections between the injection intervals and the monitor intervals. The absence of any cross-hole pressure responses was due to a combination of the limited number of cross-hole fracture connections and the inability to isolate discrete fractures in the boreholes. Fracture modeling indicated that at the scale of the radial boreholes (3 to 10 m), cross-hole testing needs to be analyzed using discrete fracture methods.

The BRFA is located in the densely welded, crystal-poor middle nonlithophysal zone (Tpcpmn) of the Tiva Canyon Tuff, on the east side (footwall) of the Bow Ridge Fault. The Bow Ridge Fault is a normal fault that has a strike/dip orientation of 180 degrees/75 degrees and about 128 m offset, which dropped younger, nonwelded, pre-Rainier Mesa tuff (Tmbt1) down to the Tpcpmn. The fault zone is about 2.7 m wide. Two boreholes were drilled from the alcove. The boreholes provided access for single-hole and cross-hole testing in the Tpcpmn, crystal-poor lower lithophysal zone (Tpcpll) of the Tiva Canyon Tuff, Bow Ridge Fault zone, and the Tmbt1. Permeability values from single-hole testing of the Tpcpmn ranged from 6.0×10^{-12} to 26.4×10^{-12} m^2; the arithmetic and geometric means were 13.9×10^{-12} and 12.2×10^{-12} m^2. Permeability values of the Tpcpll ranged from 0.6×10^{-12} to 2.0×10^{-12} m^2; the arithmetic and geometric means were 1.3×10^{-12} and 1.2×10^{-12} m^2. The three permeability values from the Bow Ridge Fault zone ranged from 8.0×10^{-12} to 15.8×10^{-12} m^2. The two permeability values from the Tmbt1 were 41.3×10^{-12} and 22.0×10^{-12} m^2.

Eleven test intervals in borehole HPF#1 indicated water redistribution. One test interval had a water-redistribution pressure of less than 50 to 100 kPa. Six test intervals had water-redistribution pressures of less than 10 to 50 kPa. Four test intervals had water-redistribution pressures that were less than 10 kPa, and the lowest was less than 5.6 kPa. Testing in the fault zone and the Tmbt1 did not indicate water redistribution. The absence of water redistribution may be because of high capillary pressures associated with the increased porosity of the nonwelded Tmbt1 or may be because the high permeability of the fault zone and Tmbt1 limited the maximum air-injection pressures.

The permeability values from cross-hole air-injection tests conducted in the BRFA were within 2 to 3 times those of the single-hole tests. The porosity estimates from cross-hole testing for the Bow Ridge Fault zone were 0.13 and 0.20; for the Tmbt1, the porosity estimate was 0.27. Comparison of the BRFA Tpcpmn permeability values to the surface-based permeability values from the Tpcpll and Tpcpln indicated that the Tiva Canyon Tuff is isotropic. Comparison of the BRFA Tpcpll permeability values and the surface-based permeability values from the Tpcpll indicated that the Tpcpll may be anisotropic and have a horizontal to vertical ratio of up to 29:1. Cross-hole tracer testing in the Bow Ridge Fault zone resulted in effective porosity values that were larger than the porosity values from air-injection testing. Some part of the increased effective porosity values may be due to adsorption of SF_6.

The UPCA is located in the moderately welded, crystal-poor lower nonlithophysal columnar subzone (Tpcplnc) of the Tiva Canyon Tuff. One borehole penetrated the Tpcplnc and two crystal-poor vitric subzones (Tpcpv1 and Tpcpv2) of the Tiva Canyon Tuff. A second borehole penetrated the Tpcplnc and the crystal-poor lower nonlithophysal hackly subzone (Tpcplnh) of the Tiva Canyon Tuff. Permeability values of the Tpcplnc ranged from 0.02×10^{-12} to 2.0×10^{-12} m^2; the arithmetic mean was 0.7×10^{-12} m^2 and the geometric mean was 0.3×10^{-12} m^2. Permeability values of the Tpcpv ranged from 0.4×10^{-12} to 57.0×10^{-12} m^2; the arithmetic mean was 16.5×10^{-12} m^2 and the geometric mean was 7.0×10^{-12} m^2. Permeability values of the Tpcplnh ranged from 0.1×10^{-12} to 12.0×10^{-12} m^2; the arithmetic mean was 3.7×10^{-12} m^2 and the geometric mean was 2.1×10^{-12} m^2. The relatively large permeability values of the Tpcpv subzones compared to the values for the Tpcpln indicated fracturing in the less welded Tpcpv subzones.

Twenty-two test intervals in the UPCA indicated water redistribution. Two of the test intervals indicated water-redistribution pressures of less than 50 to 100 kPa. Fourteen of the test intervals indicated

water-redistribution presssures of less then 10 to 50 kPa. Six test intervals indicated water-redistribution pressures of less than 10 kPa, and the lowest was less than 5.2 kPa.

Comparison of the UPCA permeability values from the Tpcplnh with the surface-based permeability values from the Tpcplnh indicated that the hackly zone may be anisotropic and have a horizontal to vertical ratio of about 8:1, depending on which of the surface-based permeability values was used for comparison. Comparison of the UPCA permeability values from the Tpcplnc to the surface-based permeability values from the Tpcplnc indicated that the columnar zone may be anisotropic and have a horizontal to vertical ratio of as much as 37:1, depending on which of the surface-based permeability values was used for comparison. Despite the predominance of vertical fracturing in the Tiva Canyon tuff (S.C. Beason, U.S. Bureau of Reclamation, written commun.,1996), the results did not indicate that the Tpcpln vertical permeability was greater than its horizontal permeability. Comparison of the UPCA permeability values from the Tpcpv to the surface-based permeability values from the Tpcpv (two test intervals) indicated that the Tpcpv is anisotropic and had a vertical to horizontal ratio of about 79:1. Comparison of the UPCA permeability values with the surface-based permeability values needs to account for the fact that the surface-based testing indicated statistically significant differences between the four surface-based boreholes (LeCain, 1997). Therefore, the fact that permeability values from a single ESF alcove agreed with some of the surface-based permeability values and not others is not surprising. Differences in the test interval depths may account for some of the variance.

REFERENCES CITED

Carslaw, H.S., and Jaeger, J.C., 1959, Conduction of heat in solids: London, Oxford University Press, 329 p.

Forchheimer, P., 1914, Hydraulik, Chapter 15: Leipzig and Berlin, p. 116–118.

Hvorslev, M.J., 1951, Time lag and soil permeability in ground-water observations: Vicksburg, Miss., U.S. Army Corps of Engineers, Waterways Experiment Station, Bulletin 36, 47 p.

Jacob, C.E., 1946, Drawdown test to determine effective radius of artesian well: American Society of Civil Engineers Transactions, Paper 2321, p. 1047–1070.

LeCain, G.D., 1995, Pneumatic testing in 45-degree-inclined boreholes in ash-flow tuff near Superior, Arizona: U.S. Geological Survey Water-Resources Investigations Report 95–4073, 27 p.

LeCain, G.D., 1997, Air-injection testing in vertical borehole in welded and nonwelded tuff, Yucca Mountain, Nevada: U.S. Geological Survey Water-Resources Investigations Report 96–4262, 33 p.

Lennox, D.H., 1966, Analysis and application of step-drawdown test: American Society of Civil Engineers Proceedings, Journal of the Hydraulics Division, v. 92, no. 6, p. 25–47.

Noman, R., and Archer, J.S., 1988, High-velocity gas flow in liquid-saturated porous media and its visualization: Journal of Canadian Petroleum Technology, v. 27, no.3, p. 64–69.

Ramey, H.J., 1982, Well-loss function and the skin effect: Geological Society of America, Special Paper 189, p. 265–271.

Rattray, G.W., Striegl, R.G., and Yang, I.C., 1995, Adsorption of sulfur hexafluoride onto crushed tuffs from the Yucca Mountain area, Nye County, Nevada: U.S. Geological Survey Water-Resources Investigations Report 95–4057, 29 p.

Van Golf-Racht, T.D., 1982, Fundamentals of fractured reservoir engineering: New York, Elsevier Scientific Publishing Company, p. 318–319.

☆ U.S. GOVERNMENT PRINTING OFFICE: 1998—673-083 / 20026 Region 8